

Intercomparison of the Performance of Operational Ocean Wave Forecasting Systems with Buoy Data

JEAN-RAYMOND BIDLOT

European Centre for Medium-Range Weather Forecasts, Reading, United Kingdom

DAMIAN J. HOLMES

Ocean Application Branch, Met Office, Bracknell, United Kingdom

PAUL A. WITTMANN

Models and Data Department, Fleet Numerical Meteorology and Oceanography Center, Monterey, California

ROOP LALBEHARRY

Meteorological Research Branch, Meteorological Service of Canada, Downsview, Ontario, Canada

HSUAN S. CHEN

National Centers for Environmental Prediction, Camp Springs, Maryland

(Manuscript received 7 March 2001, in final form 22 October 2001)

ABSTRACT

The monthly exchange of ocean wave model data has successfully been taking place among five operational weather centers. The data are compared with observations obtained from moored buoys and platforms. The analysis of 3 yr of data has helped to quantify the global and regional skills, strengths, and weaknesses of the different ocean wave forecasting systems. Since the quality of ocean wave forecasts is intrinsically linked to the quality of the forcing wind fields, it is not surprising to find that the center with the lowest wind speed errors also has the lowest wave height errors. The benefit of using a third-generation Wave Model (WAM), for example, is not so tangible in terms of wave height statistics but it is definitively evident in terms of peak periods. Even though WAM has proved to be well suited for global wave forecasting, it is also clear that research is still needed to reduce the model tendency to underpredict some storms when it is forced by operational global wind fields. It appeared that assimilating altimeter wave heights has a positive impact on the model performance. It is also argued that the height of the wind speed observations should be taken into account when assimilating the data or simply when evaluating model performance since it might otherwise introduce a systematic negative bias into the analysis. Last, this exchange of data should continue and possibly extend to other forecasting centers as a tool for model developers but also as a continuous reference for marine forecasters.

1. Introduction

Any operational weather center involved in wave prediction should have some form of quality monitoring of its products. For quite some time now, operational weather centers have systematically exchanged statistical information (scores) in an attempt to further diagnose the quality of their atmospheric model; however, prior to the end of 1995, no systematic comparative study of the different wave forecasting systems existed.

In the past, there have been some efforts to evaluate

the quality of hindcast wave products. This is particularly true when new model developments took place. The typical performance of early global wave models was summarized by Cardone (1987), Zambresky (1987, 1989), and Clancy et al. (1986). More recent evaluations of the operational performance of the third-generation Wave Model (WAM) can be found in Khandekar and Lalbeharry (1996), Wittmann et al. (1995), and Janssen et al. (1997). In an attempt to derive as much information as possible on their system, Janssen et al. also used *European Remote Sensing Satellite-1 (ERS-1)* altimeter data. Moreover, they compared forecasts with the corresponding analyses by introducing scores similar to those used for atmospheric fields.

Corresponding author address: Dr. Jean-Raymond Bidlot, ECMWF, Shinfield Park, Reading RG2 9AX, United Kingdom.
E-mail: jean.bidlot@ecmwf.int

Satellite data are another valuable source of wave observations, albeit they are not always independent and sometimes come with errors that are harder to understand. Earlier work by Romeiser (1993) and the more recent comprehensive study of Bauer and Staabs (1998) have nevertheless shown the relative good quality of both model and the latest satellite data [Ocean Topography Experiment (TOPEX), ERS].

The combined use of in situ (buoys) and satellite wave observations has now become a diagnostic tool of surface winds via the integrating effect of a wave model. Bearing in mind the imperfections of any wave model, the quality of the surface winds from the European Centre for Medium-Range Weather Forecasts (ECMWF) 15-yr reanalysis (ERA) was examined by forcing WAM with those winds (Sterl et al. 1998) and comparing the results with buoy and altimeter data. It is also done on a routine basis for the monitoring of the ECMWF forecasting system (Janssen et al. 2000a).

A systematic comparison of wave model results with other models is not often reported. It is usually confined to the initial phase of a new model implementation or when different models are compared in order to select one for operational production. Earlier work on operational North Sea predictions (Bouws et al. 1986, 1996; Günther et al. 1984) had shown how useful these comparisons could be. Therefore, in 1995, as a first step toward a more comprehensive comparison of operational wave forecasting systems, a group of wave modelers from different meteorological centers agreed to exchange wave model results (analyses and forecasts) at selected locations for which wave and surface wind information can easily be obtained. This exercise provided the participants and possibly the marine forecasters with a regular diagnostic tool for ocean wave forecasting system(s). The methodology and preliminary results of this data exchange were illustrated in Bidlot et al. (1998) and in Bidlot and Holt (1999). In this follow-up paper, the evaluation of data obtained from a 3-yr period (December 1996–December 1999) is presented.

Five centers are currently participating in the comparison. The implementation of their wave forecasting system is briefly described in section 2. The wind and wave observations are obtained from moored buoys and fixed platforms for which data are made available to the meteorological community via the Global Telecommunication System (GTS). The required data processing of these observations is summarized in section 3. Results from the statistical comparison are presented in section 4. The following section comments on some of the aspects that were illustrated in the previous sections. The paper concludes by stressing the need for the continuation and development of this data exchange.

2. Wave models

In late 1995, the ECMWF, the Met Office (formerly referred to as UKMO), the U.S. Navy's Fleet Numerical

Meteorology and Oceanography Center (FNMO), and the Atmospheric Environment Service (AES), now called the Meteorological Service of Canada (MSC), started a project aimed at exchanging wind and wave model data at given geographical points. They were joined, in May 1996, by the National Centers for Environmental Prediction (NCEP). Apart from a different atmospheric model yielding the necessary surface wind forcing, each center has a different wave model and/or a different implementation of the same original model. A basic description of each system is given below and is summarized in Table 1. More details are given in Bidlot et al. (2000).

a. The ECMWF wave model

The WAM was developed in the mid 1980s by an international group of wave modelers (Komen et al. 1994). Since then, it has been installed at many institutions around the world. At ECMWF, the WAM is in constant evolution. It has been implemented for two regions, one global and the other a higher-resolution version for the seas around Europe (Janssen et al. 1997; Bidlot et al. 1997).

The parallel version of the global model was introduced in December 1996. It has an effective resolution on the order of 55 km by making use of an irregular latitude–longitude grid (Bidlot and Holt 1999). Before July 1998, only one daily 10-day global wave forecast was obtained. It started from the 1200 UTC analysis and was forced by 10-m winds at 6-hourly intervals from the ECMWF atmospheric model output (Bengtson 1999; Janssen et al. 1997). The analysis was obtained from the previous one, updated by running the wave model with analyzed 10-m winds and blending the model data with ERS altimeter wave height observations. The scheme is based on the optimum interpolation scheme developed by Lionello et al. (1992). During this period, changes to the atmospheric model were also made. Generally, those modifications were found to have positive impacts on the quality of the surface winds and thus on the waves (Janssen et al. 2000a; Bidlot et al. 2000).

Since 29 June 1998, the wave model has been directly coupled to the atmospheric model (Janssen et al. 2000b). In this configuration, updated winds are provided hourly to the wave model subroutine that returns to the atmospheric model an update of the ocean roughness via a Charnock parameter field. This feedback is intended to model the effect of wave generation on surface stress (Janssen 1989, 1991). It was shown to be beneficial in improving global forecast scores (Janssen et al. 2000a; Janssen 2000). Two forecasts are produced daily from the 1200 UTC analysis and from the 0000 UTC short-cutoff analysis; however, only forecasts based on the 1200 UTC analysis are disseminated to users. For this reason, we will only use the forecasts based on the 1200 UTC analysis for this comparison.

TABLE 1. Wave model descriptions (1997–99).

	ECMWF	Met Office	FNMOG	AES	NCEP
Model	WAM 4.0	Second generation	WAM 4.0	WAM 4.0	WAM 4.0
Domain	Global	Global	Global	Atlantic and Pacific, north of 25°N	Global
Grid	55 km × 55 km	0.833° × 1.25° ^a	1.0° × 1.0°	1.0° × 1.0°	2.5° × 2.5°
Spectral discretization	25 frequencies, 12 directions	13 frequencies, 16 directions	25 frequencies, 24 directions	25 frequencies, 24 directions	25 frequencies, 12 directions
First frequency (Hz)	0.042	0.042	0.033	0.042	0.042
Last frequency (Hz)	0.411	0.324	0.330	0.411	0.411
Wave physics	Shallow water	Deep water ^b	Deep water	Deep water	Deep water
Wind	Coupled to T319 10-m winds	Lowest sigma level NWP model	Wind stress T159 NOGAPS	GEM 10-m winds Atlantic regional and Pacific global model	Lowest sigma level wind corrected to 10 m
Wind input	Hourly	Hourly	3-hourly	3-hourly	3-hourly
Altimeter data	Yes	Yes	No	No	Yes ^c
Ice edge	SST	Sea ice analysis	Sea ice analysis	Sea ice analysis	None
Start of forecast	0000 and 1200 UTC	0000 and 1200 UTC			
Forecast range (days)	10	5	6	2	3

^a In May 1999, increase in resolution to 60 km at midlatitude.

^b In May 1999, shallow water.

^c Assimilate buoy data as well since Feb 1998.

b. The Met Office wave model

The operational wave model run at the Met Office is a second-generation model based on the wave model first developed and described by Golding (1983), although there has been a continuous program of development since its initial implementation (Holt 1994).

The global model run consists of a 12-h hindcast, during which assimilation of *ERS-2* radar altimeter measurements of significant wave height is performed, followed by a 5-day forecast.

The Met Office wave data assimilation scheme works in a similar manner to that of the ECMWF. Each takes observations of wave height and surface wind speed and calculates the necessary changes to the model wave spectrum, so that the model wave height is “nudged” closer to the observed value (Holt 1997).

c. The FNMOG wave model

FNMOG employs both global and regional implementations of WAM 4.0. (Wittmann and Clancy 1994). The FNMOG global WAM is forced by surface wind stress at 3-h intervals from the U.S. Navy’s Operational Global Atmospheric Prediction System (NOGAPS) NWP model (Hogan and Rosmond 1991). Currently, the FNMOG WAM does not assimilate wave measurements; the model is initialized from the 3-h forecast of the previous run.

FNMOG maintains many regional implementations of WAM 4.0, some of which are nested within the global WAM depending on the existence of open-ocean boundaries (Wittmann and Pham 1999).

FNMOG plans to replace WAM 4.0 with “WAVE-

WATCH III” (Tolman 1999), in August 2001, as part of a larger operational migration from a Cray C90 computer to an SGI O3K computer.

d. The AES WAM–atmospheric model system

The Canadian Meteorological Centre (CMC) of AES implemented the WAM cycle 4 in February 1996, replacing the first-generation Canadian spectral ocean wave model. Two regional versions of the WAM were implemented: one for the northwest Atlantic Ocean and the other for the northeast Pacific Ocean.

Both regional WAMs were initially driven by 10-m winds obtained from the two different operational NWP models in use at the CMC. The Atlantic WAM was originally forced by winds from the Regional Finite Element (RFE) model. On the other hand, the Pacific WAM was forced by winds generated by the medium-range global Spectral Finite Element (SEF) model (Ritchie and Beaudoin 1994).

The Global Environmental Multiscale (GEM) model replaced the RFE model as the regional model on 24 February 1997 (Côté et al. 1998a,b). On 18 June 1997, a new global 3D variational data assimilation (3DVAR) analysis (Gauthier et al. 1999) replaced the SEF-driven global optimum interpolation analysis, and in September 1997 the 3DVAR system was implemented for the GEM regional analyses (Laroche et al. 1999). In October 1998, the SEF model was replaced by the global GEM model with the same uniform grid resolution as in the SEF model.

e. The NCEP operational global ocean wave model

From October 1994 through February 2000, WAM cycle 4 was the NCEP operational global wave model (Chen 1995). The model was modified to accommodate an everchanging ice edge and to assimilate buoy and ERS-2 altimeter wave data (since February 1998). In both cases, a successive correction scheme for data assimilation was employed.

The lowest sigma layer winds from the NCEP analysis and winds from the Aviation Model (AVN) runs of the global spectral model are adjusted to a height of 10 m by using a logarithmic profile and are used to drive the surface ocean waves. Analysis wind fields from the previous 12 h at 3-h intervals are used for a 12-h wave hindcast and AVN at 3-h intervals for the wave forecasts.

Note that as a result of a recent installment of an IBM RS/6000 SP computer system at NCEP, a third-generation wave model, WAVEWATCH III (Tolman 1999), which utilizes parallel programming and has different wave physics and a different numerical scheme, has replaced the National Oceanic and Atmospheric Administration's (NOAA) WAM as the NOAA operational global wave model since February 2000.

f. Model summary

Table 1 summarizes the key differences and similarities among the different operational systems. All centers use the WAM cycle 4, except the Met Office, which has its own second-generation wave model. AES actually runs two regional models, one for the North Atlantic and one for the North Pacific with a southern boundary at 25°N. The ECMWF wave model is now coupled to its atmospheric model, which supplies surface winds every hour. The other implementations of WAM are forced by winds updated every 3 h, and the Met Office wave model uses hourly values of surface winds. ECMWF, Met Office, and NCEP incorporate ERS-2 altimeter data in their analyses.

3. Wave and wind data

Sea state and ocean surface meteorological observations are routinely collected by several national organizations via networks of moored buoys and platforms deployed in their near- and offshore regions [the word buoys is used for moored buoys or platforms since their observations are reported under the same World Meteorological Organization (WMO) header as an automatic "synop" ship]. The geographical coverage of the data is still very limited, and at the present wave model resolution, only a small number of all these buoys are within the model grids. Nevertheless, about 40 buoys can be selected that are well within the grid of each model, in relatively deep water as most global wave models are set up as deep water models,

and that have a high rate of data availability and reliability. Figure 1 shows the location of all buoys used in this comparison.

The buoy data are transferred continuously via the GTS to most national meteorological centers and are usually archived locally. Therefore, collocations between these observations and the corresponding model values interpolated to the buoy locations can simply be obtained. A direct comparison between model values and buoy observations is undesirable as measurements may still contain erroneous data points. Furthermore, model and observed quantities represent different temporal and spatial scales.

From the buoy records, monthly time series are reconstructed and used to perform a basic quality check on the data. This quality check procedure will only keep values that are within an acceptable physical range, will try to detect faulty instruments by removing all constant records 1 day long or more, and will remove outliers by looking at the deviation from the mean of each monthly data record and from the deviation from one hourly value to the next. Spatial and temporal scales are made comparable by averaging the hourly observations in time windows of 4 h centered on the synoptic times. GTS data are, unfortunately, provided with some truncation. Wave heights are rounded to the closest 0.1 m, peak frequencies to the closest second, and wind speed to the closest meter per second. Averaging will diminish the effect of these truncations. The resulting errors for wave data are well within what can be expected from buoy measurements (Monaldo 1988). It is unfortunate, however, that wind speed observations are encoded with such a large truncation error (up to 0.5 m s⁻¹) since they still need to be adjusted to 10 m (see below).

This quality check procedure is run at ECMWF. For completeness, the ECMWF collocation files also include the raw synoptic (unaveraged) observations. Other centers have built similar buoy-model collocations or have agreed to provide corresponding model values at as many buoy locations as possible (Fig. 1). Every month, each participating center creates files that contain model monthly time series of 10-m wind speed and direction, wave height, and wave peak period at the selected buoy locations. It was agreed to look at the analysis and forecasts up to day 5 (when available; see Table 1). These files are transferred via FTP to the Met Office server, where they are combined with the observations processed by ECMWF. In the future, some of the results should be made available by posting them on the Internet.

It is the responsibility of each individual center to retrieve the combined files from the Met Office server. The statistical analysis of the data is left to each center, which may decide to look at it from their own perspective. However, ECMWF has a semiautomatic procedure to analyze the monthly results from which tables and summary graphs are produced. These tables and graphs are also available every month from the Met

1	21004	JAPAN	7.5m	JMA Shikoku South	E,U,F,N	19	46005	USWC	5.0m	NDBC Washington	E,U,F,N,A
2	22001	JAPAN	7.5m	JMA Ryukyu Islands	E,U,F,N	20	46006	USWC	5.0m	NDBC SE Papa	E,U,F,N,A
3	41001	USEC	5.0m	NDBC East Hatteras	E,U,F,N,A	21	46035	NPC	5.0m	NDBC Bering Sea	E,U,F,N,A
4	41002	USEC	5.0m	NDBC South Hatteras	E,U,F,N,A	22	46036	USWC	5.0m	CMEDS South Nomad	E,U,F,N,A
5	41010	USEC	5.0m	NDBC Cape Canaveral East	E,A	23	46059	USWC	5.0m	NDBC California	E,F,N,A
6	42001	GM	10.0m	NDBC Mid Gulf of Mexico	E,U,F,N	24	46184	NPC	5.0m	CMEDS North Nomad	E,U,F,N,A
7	42003	GM	10.0m	NDBC Eastern Gulf of Mexico	E,U,F,N	25	51001	HW	5.0m	NDBC Hawaii North West	E,U,F,N
8	44004	USEC	5.0m	NDBC Hotel	E,U,F,N,A	26	51002	HW	5.0m	NDBC Hawaii South West	E,U,F,N
9	44008	USEC	5.0m	NDBC Nantucket	E,U,F,N,A	27	51003	HW	5.0m	NDBC Hawaii West	E,U,F,N
10	44011	USEC	5.0m	NDBC Georges Bank	E,U,F,N,A	28	51004	HW	5.0m	NDBC Hawaii South East	E,U,F,N
11	44137	CANEC	5.0m	CMEDS East Scotia slope	E,F,A	29	62029	NEATL	4.5m	UKMO K1	E,U,F,N
12	44138	CANEC	5.0m	CMEDS SW Grand Bank	E,F,N,A	30	62081	NEATL	4.5m	UKMO K2	E,U,F,N
13	44141	CANEC	5.0m	CMEDS Laurentian Fan	E,F,N,A	31	62105	NEATL	4.5m	UKMO K4	E,U,F,N
14	44142	CANEC	5.0m	CMEDS Lahave Bank	E,F,N,A	32	62106	NEATL	4.5m	UKMO RARH	E,F
15	46001	NPC	5.0m	NDBC Gulf of Alaska	E,U,F,N,A	33	62108	NEATL	4.5m	UKMO K3	E,U,F,N
16	46002	USWC	5.0m	NDBC Oregon	E,U,F,N,A	34	62163	NEATL	4.5m	UKMO Brittany	E,F,N
17	46003	NPC	5.0m	NDBC Aleutian Peninsula	E,U,F,N,A	35	63111	NSEA	10.0m	UKMO Platform Beryl	E,U,F,N
18	46004	NPC	5.0m	CMEDS Middle Nomad	E,U,F,N,A	36	64045	NEATL	4.5m	UKMO K5	E,F,N

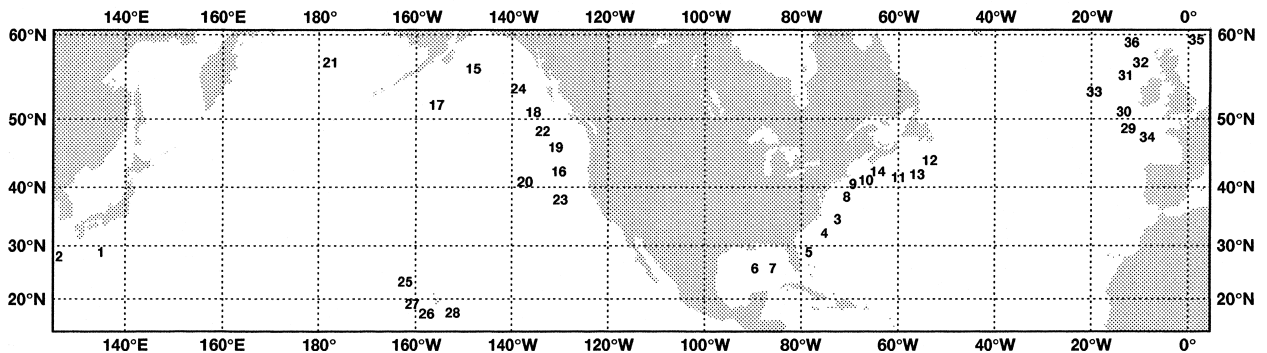


FIG. 1. Locations of all buoys used in the comparison. In the accompanying table, the five-digit WMO buoy identifier is followed by the abbreviated name of the region to which it belongs when compiling statistics per area: Hawaii (HW), Japan (JAPAN), the North Pacific (NPC), U.S. west coast (USWC), U.S. east coast (USEC), Gulf of Mexico (GM), Canadian east coast (CANEC), the northeast Atlantic (NEATL), and the North Sea (NSEA). It is followed by the actual height of the anemometer obtained from the different data providers: the Japanese Meteorological Agency (JMA), the U.S. National Data Buoy Center (NDBC), the Canadian Marine Environmental Data Service (CMEDS), and the Met Office (UKMO). When known, the name used by the data provider or the geographical location is shown along with the first initial of each center for which model data are also available.

Office server. The same software can also be used to look at longer periods.

In this paper and in the future, statistics are compiled with quality-controlled data supplemented with a black-listing (omission) of a few data segments. The black-listing of certain stations is done each month by collecting information from the data providers (Web pages, e-mails, etc.) and by analyzing the monthly time series for suspicious behaviors that may have eluded the earlier quality control. Note that it was decided to use near-real-time GTS data instead of data compiled later by the respective data providers, presumed of better quality, since most centers generate their buoy-model collocation when model data are still directly available online for immediate comparison.

Buoy anemometers are not usually at a height of 10 m. However, the heights of the anemometers have been obtained from the data providers (Fig. 1). The wind speed statistics were produced by adjusting the buoy winds to 10 m. The steady-state neutrally stable logarithmic vertical wind profile relation is solved for the

friction velocity (u^*) assuming that the surface roughness (z_o) can be specified by the Charnock relation with a constant parameter (α) of 0.018 (Charnock 1955). In that case, the wind speed (U) at height z is given by

$$U(z) = \frac{u^*}{\kappa} \ln\left(\frac{z}{z_o}\right) \quad \text{and} \quad (1)$$

$$z_o = \alpha \frac{u^{*2}}{g}, \quad (2)$$

where κ is the von Kármán constant ($\kappa = 0.41$) and g is the acceleration of gravity. The same logarithmic profile is then used to determine the corresponding wind speed at 10 m.

4. Data products

a. Global analysis

Figure 2 shows scatter diagrams of the collocation between all buoy data and model wave heights and wind

(a)

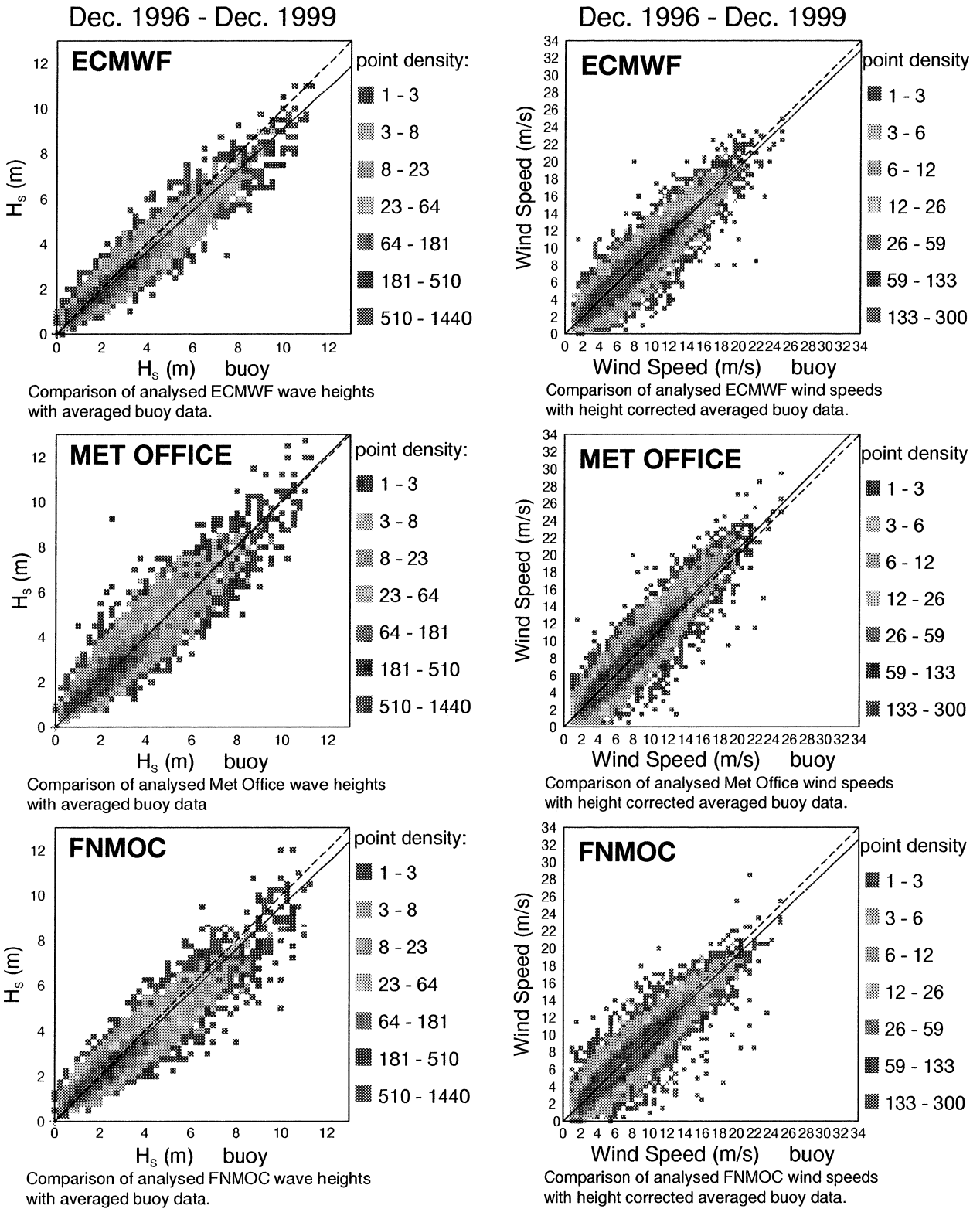


FIG. 2. (a) (b) Scatter diagrams for the 1200 UTC analyzed (left) wave heights and (right) wind speeds with respect to the averaged buoy data (see text). Buoy wind speeds were adjusted to 10 m by using a neutrally stable logarithmic wind profile. Only buoys for which ECMWF, Met Office, and FNMOC model data were available were used to produce the statistics (Fig. 1). Note that AES results are limited to buoys

(b)

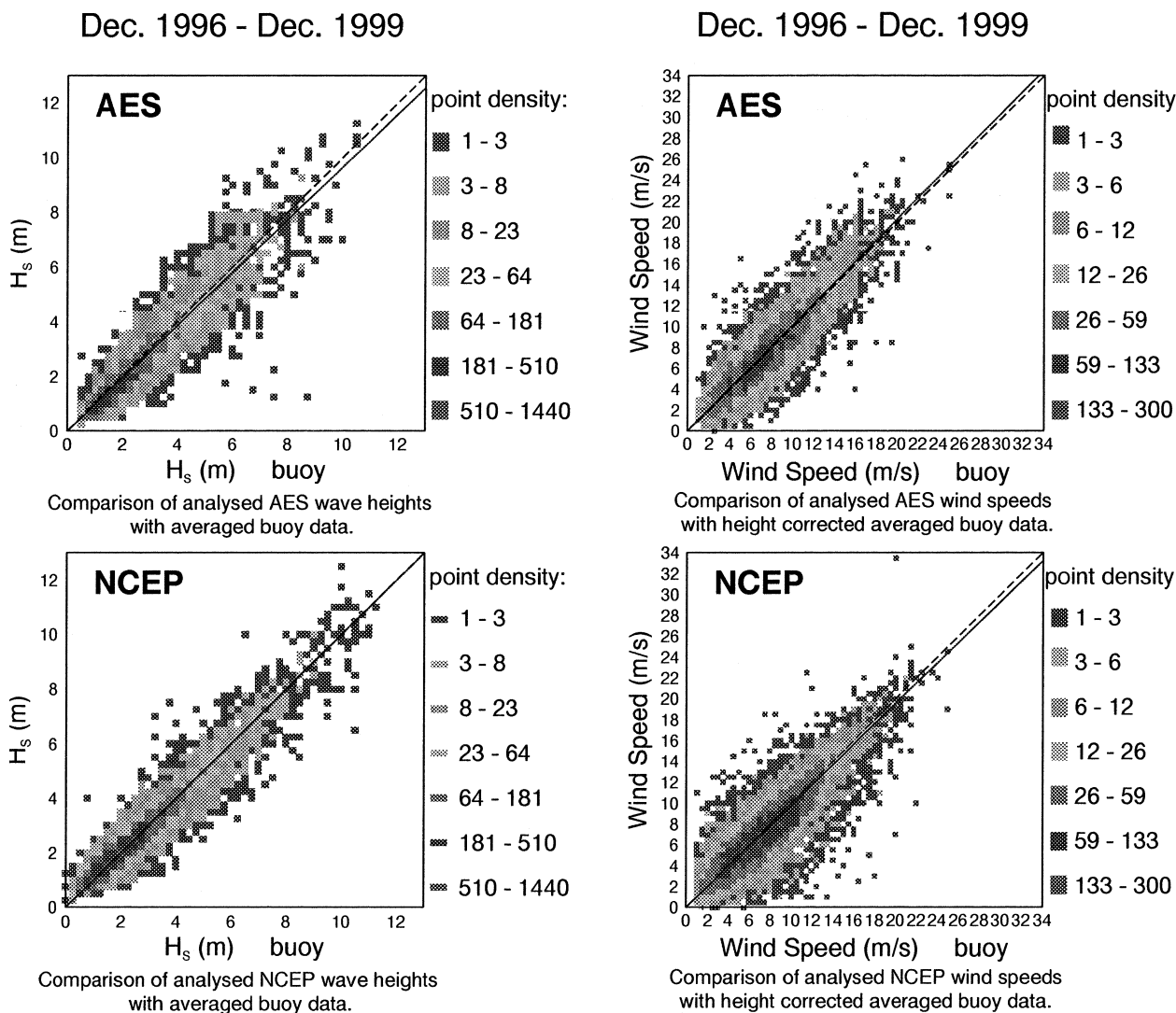


FIG. 2. (Continued) along the American coasts and NCEP has reported fewer data points than the others. The solid line is the linear fit through the origin with a slope given by the symmetric slope (see the tables). Both model and buoy data were binned into squares that are shaded according to the number of points within each square.

speeds for the 1200 UTC analysis from December 1996 to December 1999. This 3-yr period runs from the introduction of the 55-km grid in the ECMWF model to the end (almost) of the operational use of WAM at NCEP. The corresponding statistics are summarized in Tables 2 and 3. Note that for these plots, only collocation points are considered that were common to the three centers that issue 5-day forecasts (i.e., ECMWF, Met Office, and FNMOC). AES statistics are produced only with buoys along the continental United States and Canada (statistics per region are discussed below). NCEP has slightly fewer data points because of technical difficulties in exchanging all collocated data. Also, note that NCEP has been making use of buoy data in their wave model assimilation since February 1998. Similar

scatterplots and statistics can be produced for the forecast products. Figure 3 and Tables 4 and 5 present the statistics for the day 2 forecast for the same period. From the visual inspection of the scatter diagrams for the analyzed wave heights (Fig. 2), it appears that among the centers that do not assimilate buoy data, ECMWF had the smallest scatter. However, for this 3-yr period, all WAM models have a tendency to underestimate some events, ECMWF's version in particular. This impression is confirmed by the statistics displayed in Tables 2 and 3. ECMWF has indeed the smallest scatter index (standard deviation of the difference between model and buoy normalized by the buoy mean) but it has the largest negative bias (model minus buoy) and a symmetric slope of less than 1 (the slope of the linear fit where neither

TABLE 2. Analyzed wave height statistics from Dec 1996 to Dec 1999. Negative bias denotes lower model values with respect to buoy observations. The scatter index is defined as the standard deviation of the difference between model and buoy normalized by the observation mean. The symmetric slope refers to the ratio of the sum of the squares of the model results with the sum of the squares of the observations.

$t + 0$	ECMWF	UKMO	FNMOG	AES	NCEP
No. of entries	25 343	25 343	25 343	12 528	17 788
Buoy mean (m)	2.49	2.49	2.49	2.55	2.53
Bias (m)	-0.17	0.04	-0.06	-0.13	0.03
Rmse (m)	0.46	0.52	0.49	0.55	0.43
Scatter index	0.17	0.21	0.20	0.21	0.17
Symmetric slope	0.91	1.01	0.95	0.97	1.00

the observations nor the model values can be used as a reference). Not surprisingly, the scatter diagrams for the analyzed wind speed generally show a good fit between models and observations. Note that with the exception of the Met Office, all global models have a small negative global bias (recall that the wind speed data were adjusted to a height of 10 m).

The scatter diagrams for the day 2 forecast clearly illustrate the degradation of the quality of the forecasts with respect to the analysis, especially for the wind speed (Fig. 3). As discussed in Janssen et al. (1997), the apparent better fit between model waves and observations can be partly explained by the presence of swell in most wave systems. Swell is by definition composed of waves that were generated elsewhere and thus earlier in the forecast with winds of better quality or where amplitudes were corrected by previous analyses. Nevertheless, it is also known that the quality of the wave spectrum still under the direct influence of the wind (wind sea component) is intrinsically linked to the quality of the forcing winds (Janssen et al. 1997; Janssen 1998, 2000). It is therefore not surprising that the ECMWF wave forecasts are in better agreement with the buoy observations since this appears to be the case for the wind speed.

This global picture of the performance of each system should be complemented with the seasonal variation of the different statistics. The time series of the 3-month running average of the analysis and day 3 forecast wave height bias and scatter index are presented in Fig. 4 for ECMWF, the Met Office, and FNMOG. The plots clearly illustrate the seasonal variation of the error, as well as the seasonal rate of degradation of the forecasts. By comparing the analysis time series with its forecast counterpart, it also appears that the ECMWF random forecast error has on average a slower growth than the other centers. This will be confirmed when we look at forecast error growth curves in the next section.

A comparable analysis can be done for the monthly evolution of the 10-m wind speed bias and scatter index. Note, however, that the wind observations are included in the data made available to the atmospheric model assimilation. It has been recognized that buoy wind measurements are made by anemometers that are not necessarily located at 10 m above mean sea level. Some observations are crudely corrected for this height dis-

crepancy, but most of them are not. In most assimilation systems, no height correction is made to the buoy winds. The magnitude of the correction can be estimated by multiplying the buoy observation (usually obtained around 10 m) by a factor of 1.07 to adjust it to 10 m for a neutrally stable atmosphere (Smith 1988). Since the atmosphere is not necessarily stable over the areas covered by the buoy networks, implying a different wind profile from neutrally stable, this adjustment would also have errors (Zambresky 1989). Without any correction, a good analysis fit to the wind might actually result in an underestimation of the real 10-m wind since most buoy anemometer heights are around 5 m, potentially resulting in an underestimation of the wave energy generated by the local winds. For example, if the wind speeds were adjusted to 10 m for a neutrally stable atmosphere, as is done to produce Fig. 4, the wind speed bias would be reduced by about 0.5 m s^{-1} for a buoy mean wind of 8 m s^{-1} . A mean wind speed of 8 m s^{-1} with a negative bias of -0.5 m s^{-1} can result in a negative wave height bias of -0.2 m (see section 5).

Buoy measurements of the period at the peak of the one-dimensional wave spectrum (peak period) are harder to compare with model estimates because of the different methods used to determine them. For example, the Met Office model has only 13 frequency components, and the method for calculating the peak period is simply to choose the component with maximum energy. So for low frequencies, when the discretized frequency components are spread the most, the model peak period might be crudely estimated. In contrast, the FNMOG model fits a spline to the spectrum before calculating the peak period. The other models are also limited by their frequency resolution (25 bins). For example, the scatter diagrams for analyzed peak periods from ECMWF, FNMOG, and the Met Office are presented in Fig. 5 for the same collocation as in Fig. 2. Note however, that this comparison excludes the northeast Atlantic buoys since their GTS records for wave period do not use a peak period definition but rather an integrated weighted-spectral mean. A global inspection of these scatter diagrams already indicates the model tendency to overestimate the peak period (see Table 6), especially for the Met Office model. Furthermore, it appears that low buoy values are overestimated but large peak periods are underpredicted. The model overesti-

TABLE 3. Analyzed 10-m wind speed statistics from Dec 1996 to Dec 1999. Negative bias denotes lower model values with respect to buoy observations. The scatter index is defined as the standard deviation of the difference between model and buoy normalized by the observation mean. The symmetric slope refers to the ratio of the sum of the squares of the model results with the sum of the squares of the observations. The buoy wind data were adjusted to neutrally stable 10-m wind using a logarithmic vertical profile with a Charnock parameter of 0.018 [see (1) and (2)].

$t + 0$	ECMWF	UKMO	FNMOC	AES	NCEP
No. of entries	28 830	23 820	23 820	11 342	16 747
Buoy mean (m s^{-1})	7.39	7.39	7.39	7.46	7.43
Bias (m s^{-1})	-0.31	0.16	-0.37	0.03	-0.27
Rmse (m s^{-1})	1.43	1.42	1.43	1.83	1.96
Scatter index	0.18	0.18	0.18	0.23	0.25
Symmetric slope	0.97	1.03	0.96	1.02	0.98

mation of the peak period might indicate that some observed low-frequency systems are arriving later than what the models are predicting. Analysis of time series partly confirms that view; however, there are also instances where the locally generated wind sea is not as strong as observed and the peak period then points to a dominant low-frequency system.

b. Categorized global statistics

Another insight into the data can be obtained by looking at the statistics as a function of the observed quantities. In Fig. 6, the statistics were produced for all sets of model–buoy collocations with buoy data within certain bins. Note that in order to smooth out the plots, the bins overlap. The data used are the same as in the previous figures. The wave height statistics are given as a function of buoy wave height but also as a function of observed wind speed and peak period. The evolution of the wave height biases for the analysis and day 2 forecast indicates a slight overestimation for low wave height or very low wind speed and an increasing underestimation for higher wave heights or winds for both ECMWF and FNMOC. On the other hand, the Met Office wave height bias evolution is quite different with a positive forecast bias for most of the wave height and wind speed range except for the very high values and a slightly negative bias for the Met Office analysis except for low values. As a function of observed peak periods, the analysis wave height biases are fairly constant with a slight tendency at becoming more negative for larger periods. Forecast biases are less negative. In terms of scatter index, the ECMWF wave height analysis and forecasts have the lowest values over the whole observed wave height range.

The analyzed wind speed biases for ECMWF and FNMOC are negative for most of the observed wind range except for wind speeds below $4\text{--}5 \text{ m s}^{-1}$. Meanwhile, the Met Office analysis bias is quite small for most of the observed range but increases for high winds. For the day 2 forecast, all centers overestimate low wind speeds. For higher values, FNMOC has a negative bias that can be quite substantial for high wind speeds, as does ECMWF, even though the high wind speed bias is less pronounced. Meanwhile, Met Office has a small

positive bias. The analyzed wind speed scatter index is nearly identical for all three centers, whereas the day 2 forecast scatter index favors ECMWF for the full observed range.

The wave peak period can be used to point out which wave system is dominant. When compared with buoy peak periods, all centers have a tendency to predict dominant wave systems with larger peak period until about 11–13 s (the wind sea range). In contrast, lower-frequency systems (swells) are predicted with a lower peak period. Note that the noticeable difference between the Met Office and the other centers should in part be attributed to the cruder method with which the Met Office peak periods are determined. The general tendency is nevertheless the same.

c. Regional statistics and analysis of the AES system

All statistics presented so far were for all buoys combined; the same can be done by selecting a subset of buoys that are in a region with similar climatological conditions (Fig. 1). There are some regional differences in analysis and forecast performance. As mentioned in the description of the AES model, wind input for their WAM comes from different CMC atmospheric models. The effects of some of the changes to the wind input are clearly visible in the statistics when they are split between the North Pacific and the North Atlantic regions (Fig. 7). The statistics obtained from other centers can be used as references to what could be expected. The GEM model replaced the RFE model in February 1997 and its grid resolution increased to 0.22° in October 1998. These changes seem to have had little impact on the wave height bias since the model physics and grid resolution were very similar to those of the RFE model. In the Pacific, however, the mainly positive wave height bias gave way to negative bias after implementation of the global GEM model in October 1998. This underprediction is more consistent with the underprediction produced by the wind input from the regional GEM model in the Atlantic.

The statistics for the East Coast are quite different than from the West Coast. This feature is not limited to AES; in fact, all centers show similar characteristics. It is clear that even though the standard deviation of

(a)

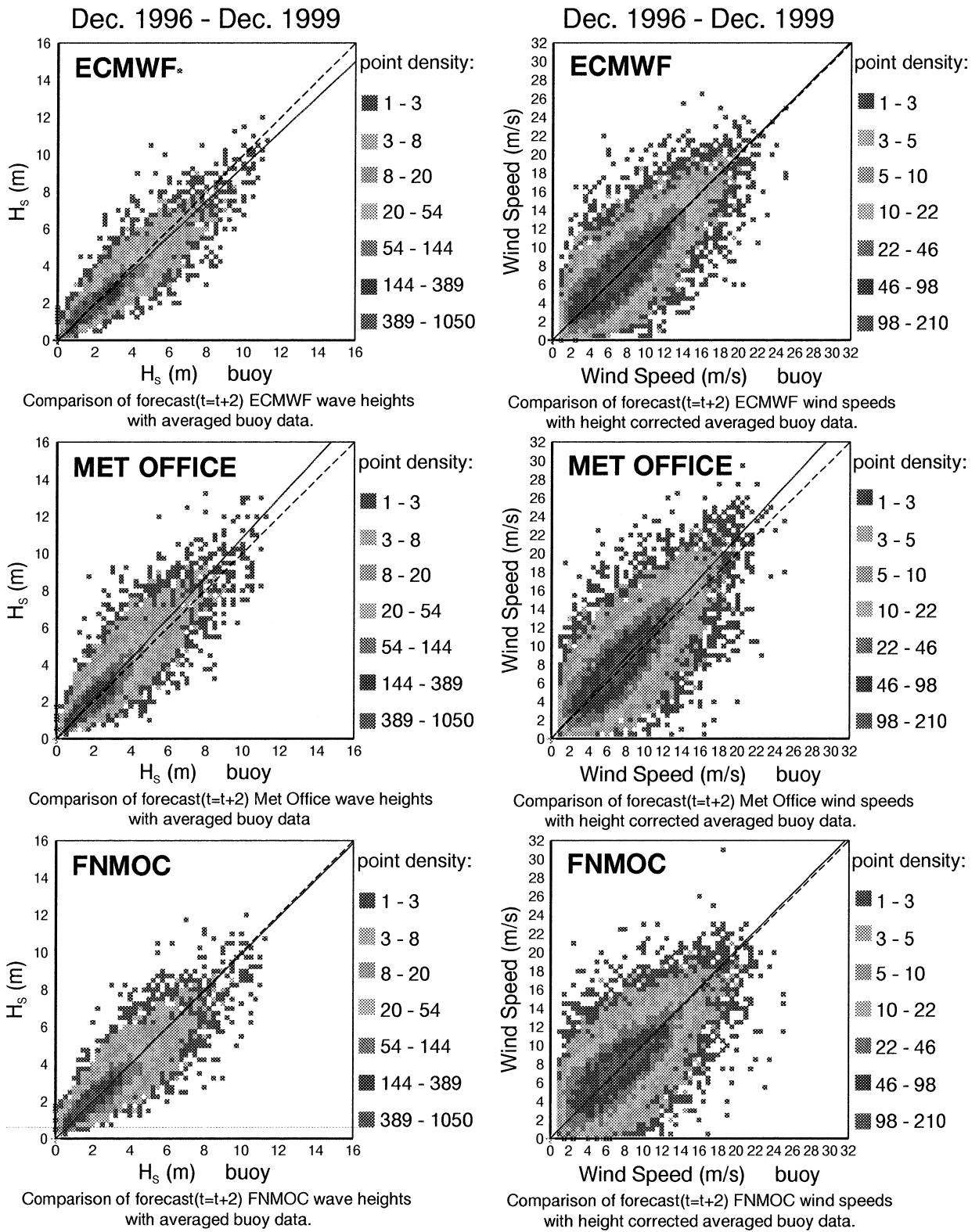


FIG. 3. Same as in Fig. 2 but for the day 2 forecasts beginning at 1200 UTC.

(b)

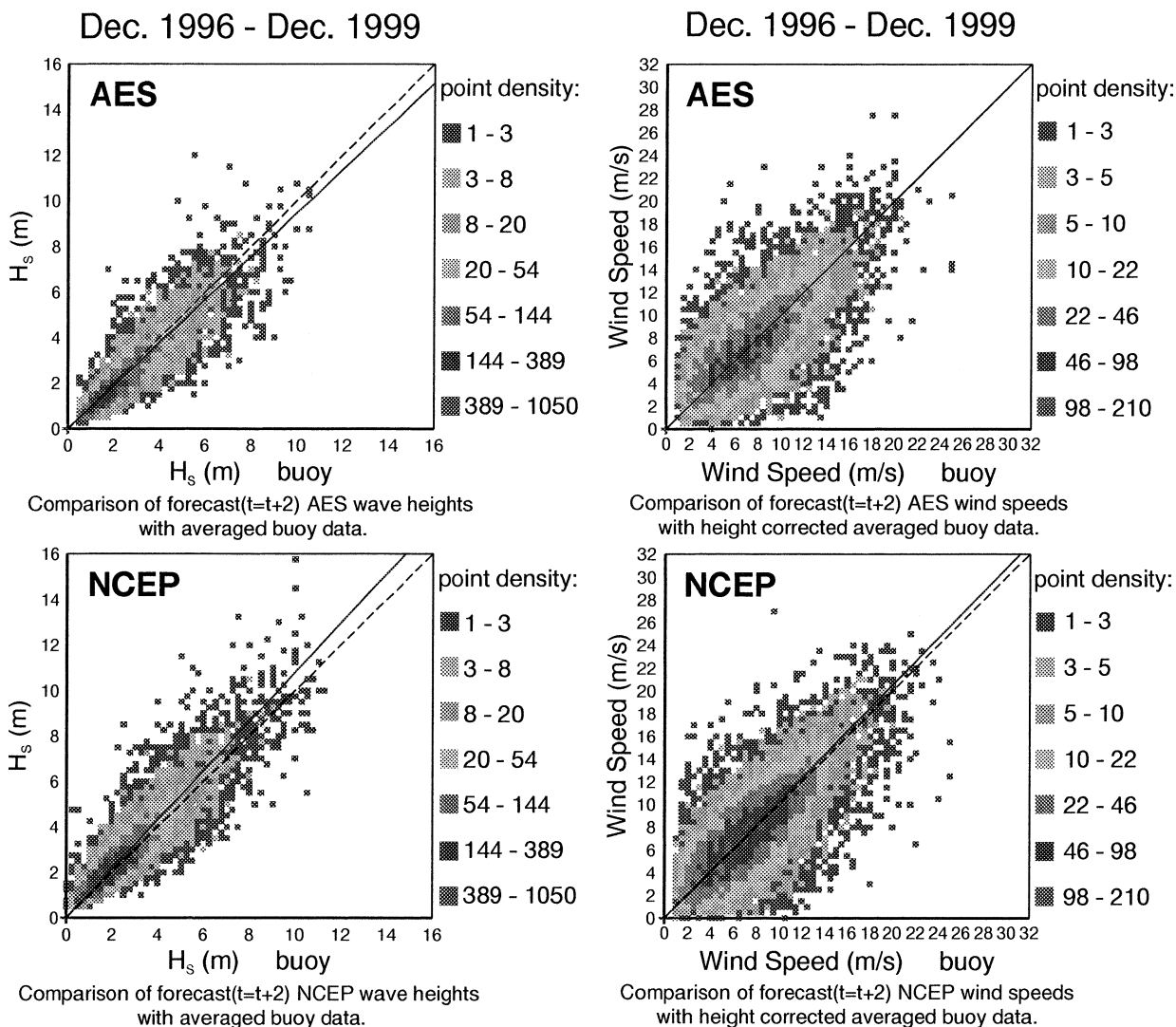


FIG. 3. (Continued)

error is less for the Atlantic buoys, wave heights are generally lower resulting in a larger relative error. Furthermore, intense fast moving disturbances are frequent along the eastern seashore (cold-air outbreaks, coastal jet intensification, rapid cyclogenesis, etc.). The effects of these systems are harder to model than well-developed midlatitude storms that regularly batter the

West Coast. Last, there are also the occasional tropical storms and hurricanes that affect the East Coast. The large wave height scatter index at the end of the summer periods (August–September) is partly attributable to some degree to these intense storms and also to swell from very distant storms in the Southern Hemisphere midlatitudes.

TABLE 4. Same as in Table 2 but for the day 2 forecasts started at 1200 UTC analyses.

$t + 2$	ECMWF	UKMO	FNMOC	AES	NCEP
No. of entries	25 334	25 334	25 343	12 508	18 161
Buoy mean (m)	2.49	2.49	2.49	2.55	2.52
Bias (m)	-0.13	0.20	0.03	-0.17	0.24
Rmse (m)	0.60	0.76	0.65	0.68	0.72
Scatter index	0.23	0.29	0.26	0.26	0.27
Symmetric slope	0.94	1.08	0.99	0.94	1.08

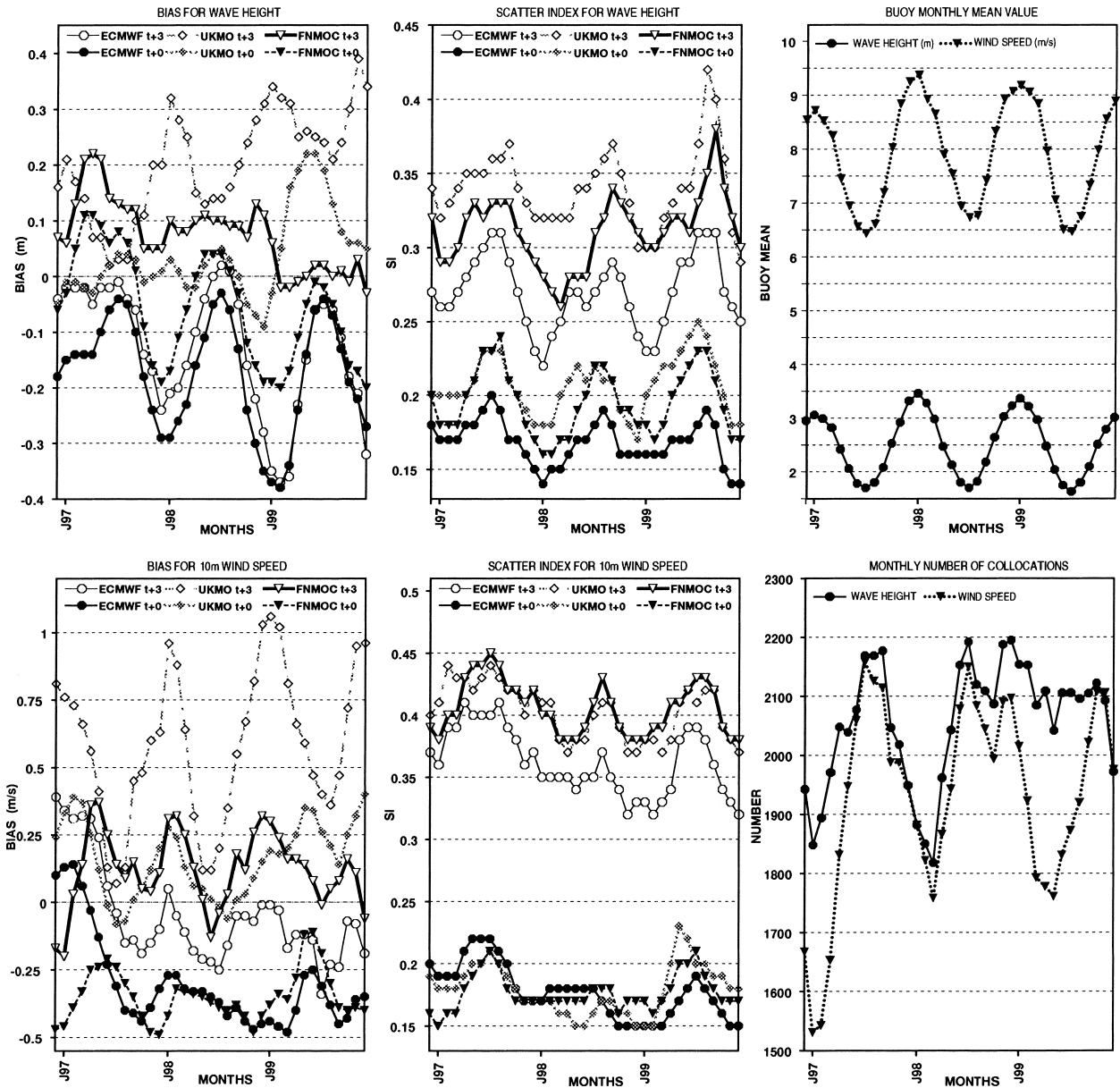


FIG. 4. Monthly time series of analysis ($t + 0$) and day 3 forecast ($t + 3$) bias and scatter index for model wave heights and 10-m winds when compared with buoy data that are common to ECMWF (solid line with circles), Met Office (dotted line with diamonds), and FNMOC (dashed line with triangles) from Dec 1996 to Dec 1999. Buoy winds were adjusted to 10 m and a 3-month running average was used to smooth out the plots. Also shown are the mean buoy observations and the number of collocations between models and buoys.

TABLE 5. Same as in Table 3 but for the day 2 forecasts started at 1200 UTC analyses.

$t + 2$	ECMWF	UKMO	FNMOC	AES	NCEP
No. of entries	23 746	23 746	23 746	11 290	17 290
Buoy mean ($m s^{-1}$)	7.39	7.39	7.39	7.47	7.41
Bias ($m s^{-1}$)	-0.02	0.56	0.09	-0.01	0.12
Rmse ($m s^{-1}$)	2.37	2.75	2.79	2.78	2.68
Scatter index	0.30	0.34	0.35	0.35	0.34
Symmetric slope	1.00	1.08	1.01	1.00	1.02

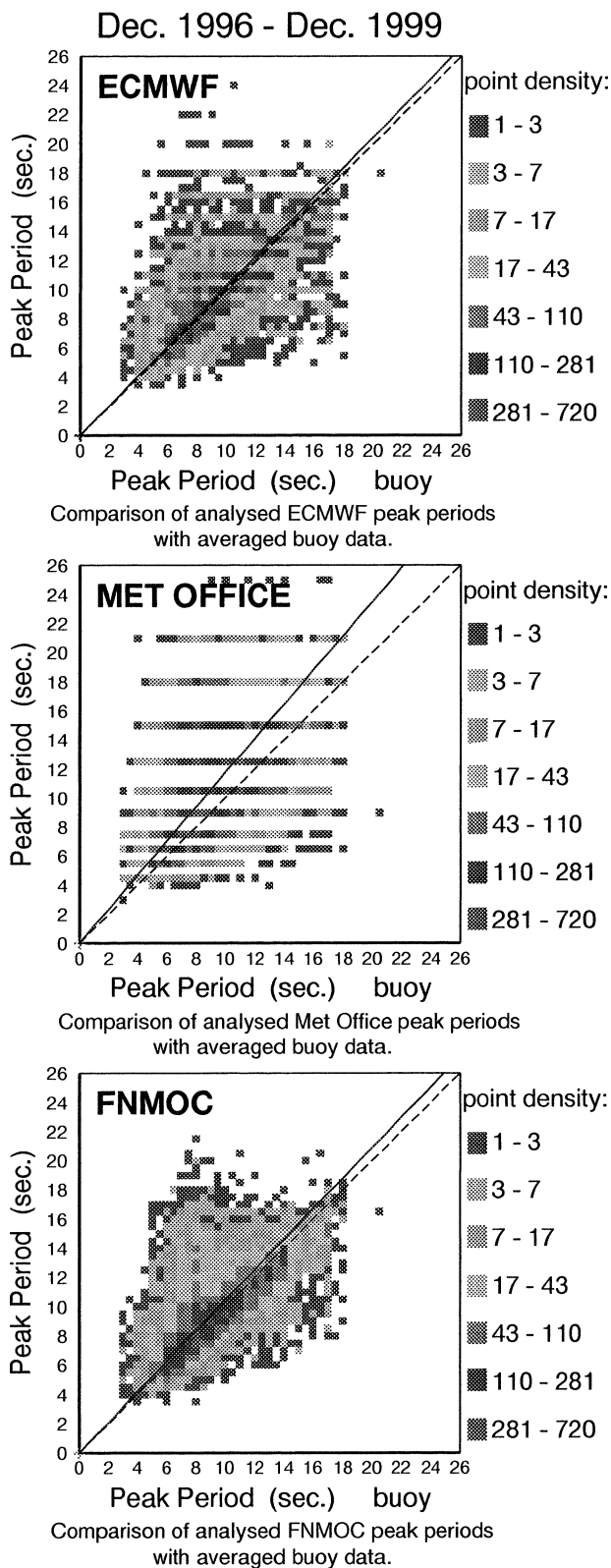


FIG. 5. Same as in Fig. 2 but for the peak period of the one-dimensional analyzed wave spectra. Please refer to the text for a description of the different methods used to derive the peak period.

TABLE 6. Same as in Table 2 but for peak periods.

$t + 0$	ECMWF	UKMO	FNMOC
No. of entries	19 665	19 665	19 665
Buoy mean (s)	9.44	9.44	9.44
Bias (s)	0.26	1.57	0.23
Rmse (s)	2.16	3.54	2.20
Scatter index	0.23	0.34	0.23
Symmetric slope	1.02	1.17	1.04

In general, both SEF and GEM models have relatively small wind speed biases in both ocean basins. The extremely large bias ($\sim 2 \text{ m s}^{-1}$) in the spring of 1997 undoubtedly was due to the absence of a spinup cycle of the regional GEM model as this bias was considerably reduced in the day 2 forecast. In terms of the wind speed scatter index, the same discussion as for the wave height scatter index applies when comparing the Atlantic with the Pacific buoy regions.

d. Regional winter and summer statistics

It is also interesting to compile regionally the other model analyses and forecasts for all winter months (December–February) and all summer months (June–August). Figure 8 displays the winter and summer month bias and scatter index evolution for buoys located around the Hawaiian Islands. This area is generally dominated by steady winds and swell as indicated by the moderate mean wave height and large mean peak period. These characteristics might explain the relatively slower and uniform wave height error growth as compared with other areas (see below). The wind speed bias evolution is quite flat as compared with the adjustment in the first day (spinup), which might be attributed to some unbalanced physics. As mentioned earlier, a direct comparison of the peak period between the different models is not possible. Nevertheless, a comparison between the summer and winter months indicates that for each center the relative errors and bias are larger in the summer, even though the wave height errors are lower then. Note that in the summer, swells around Hawaii mostly originate from the Southern Hemisphere, pointing to model error in the long swell propagation.

Swell contribution to the wave field in the North Pacific and along the west coast of North America is also important; however, waves are also generated by passing midlatitude storms. Figure 9 illustrates the kind of errors that exist for buoys in the North Pacific region. Winter and summer periods exhibit similar relative errors for wind speeds and wave heights. In term of bias, winter periods are characterized by negative analysis biases for wave heights for all WAM implementations and zero bias for the Met Office model. ECMWF has the largest negative biases. These negative biases can be connected to underestimation of some of the peaks in the wave height time series (not shown). The Met Office has no winter bias but tends to overestimate some of the events.

(a)

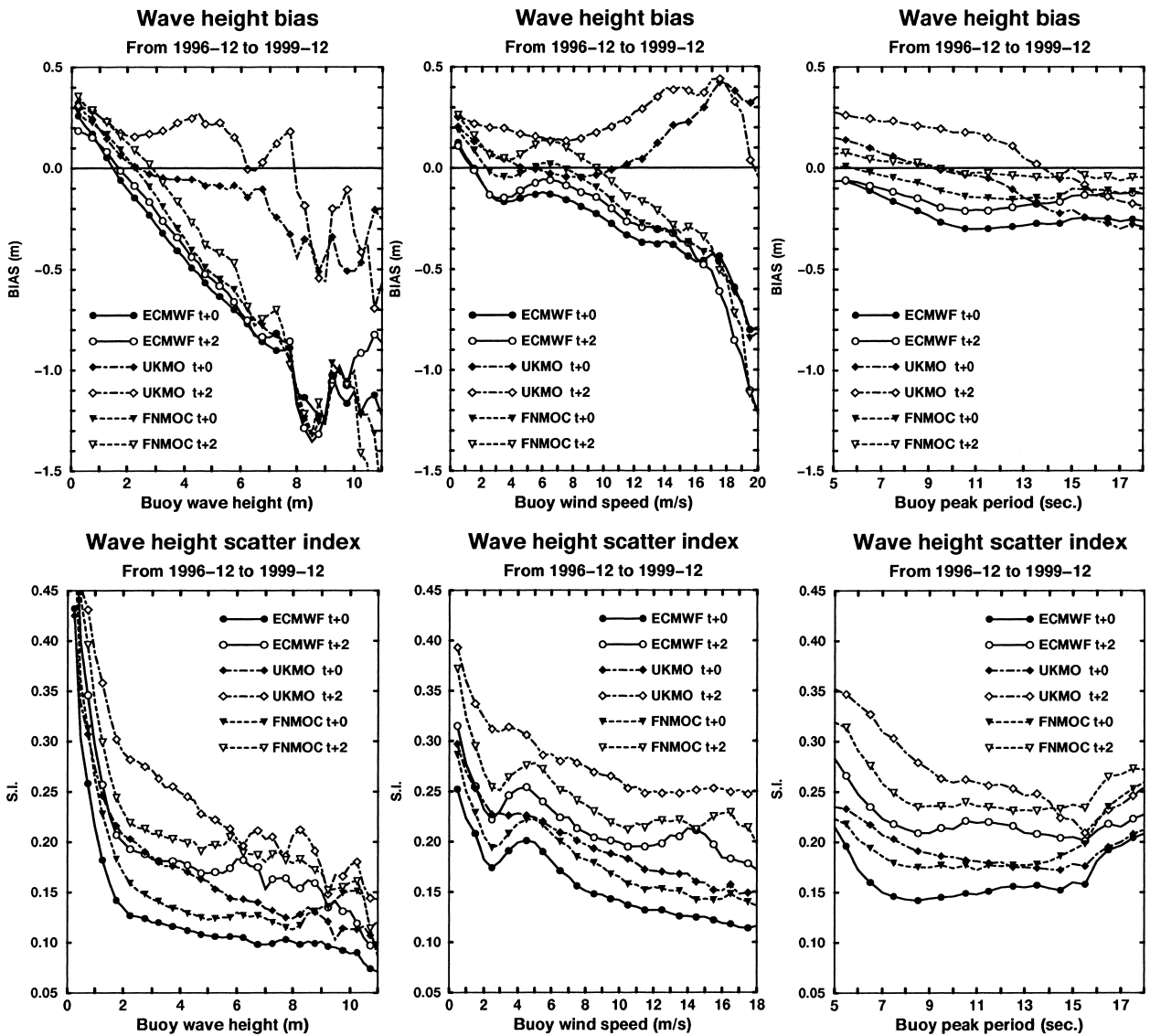


FIG. 6. (a) Wave height bias and scatter index (S.I.) as obtained when data are binned with respect to the buoy data (wave heights, wind speeds, and peak periods) for the period from Dec 1996 to Dec 1999. Note that the bins overlap. The same symbol convention as in Fig. 4 is used here. (b) Wind speed and peak period bias and S.I. as obtained when data are binned with respect to the buoy data for the period from Dec 1996 to Dec 1999. Note that the bins overlap. The same symbol convention as in Fig. 4 is used here.

Following Janssen et al. (1997), it is worth mentioning why the initial random error growth for wave heights is flatter than the error growth for wind speeds. In their paper, the authors demonstrate that the wave height error growth is partly determined by swell error growth virtually independent of forecast time and by a more dominant wind sea contribution that is directly connected to the forcing winds. The combination of both these error sources results in a slower error growth in the first stage of the forecast.

Wave climate along the U.S. and Canadian east coasts is less influenced by long swells that have propagated from afar, except in the summer when local winds are

weak. These areas are regularly subject to rapidly developing storms and frontal passages that are usually intensifying during the transition from land to sea, and are also along the tracks of occasional hurricanes. There is also the presence of the Gulf Stream that affects the airflow stability and possibly the wave growth via wave-current interaction. Under these conditions, it is not surprising that it is a more difficult area for wave modeling. Figure 10 displays the type of statistics that can be obtained from the comparison with the selected buoys along the U.S. east coast. By comparing it with statistics from buoys on the other side of the North American continent (Fig. 9) or on the other side of the

(b)

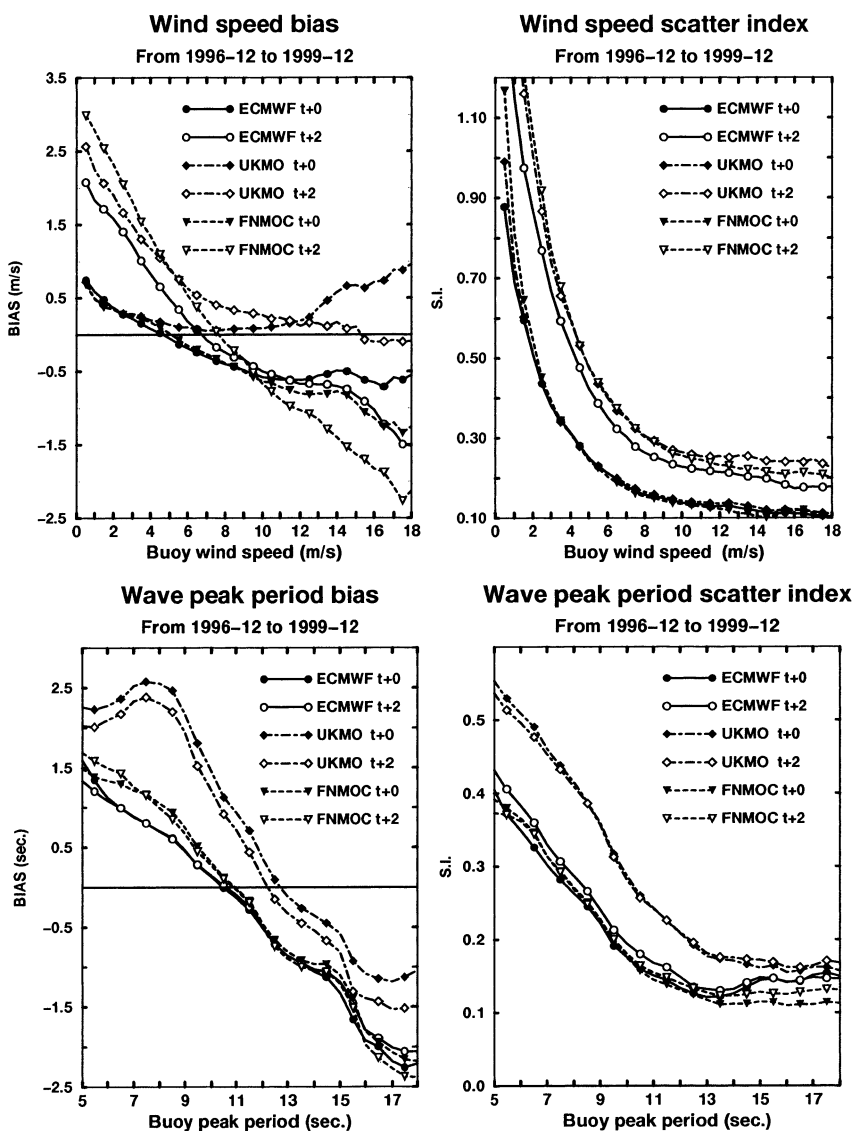


FIG. 6. (Continued)

Atlantic (Fig. 11), it is clear that in relative terms, the errors are larger. A similar conclusion can also be made from the Japanese buoy data (not shown). ECMWF, which has a clear advantage for all other regions, has a comparable scatter index for its analysis and short-range forecasts with the other centers, yet it has a larger negative bias.

Statistics for buoys on the Atlantic front of the British Isles are displayed in Fig. 11. In terms of scatter index, this region is well modeled. ECMWF and FNMOC have a tendency to underestimate maxima in the wave height time series, resulting in a systematic negative bias, while the Met Office can underestimate and overestimate depending on the circumstances. As is the case for the North Pacific, the source of the errors can be linked in

part to long swells but also to inconsistencies in the local stormy weather.

5. Discussion

It is beyond the scope of this paper to review all the different aspects of each system in order to understand the observed differences. In the 3 yr covered by this study, both atmospheric and wave models have gone through a series of changes, while some characteristics of each model have remained the same. The Met Office is still using a second-generation wave model with limited frequency and angular resolution. A comparison between second- and third-generation wave models has already been extensively covered in the past (SWAMP

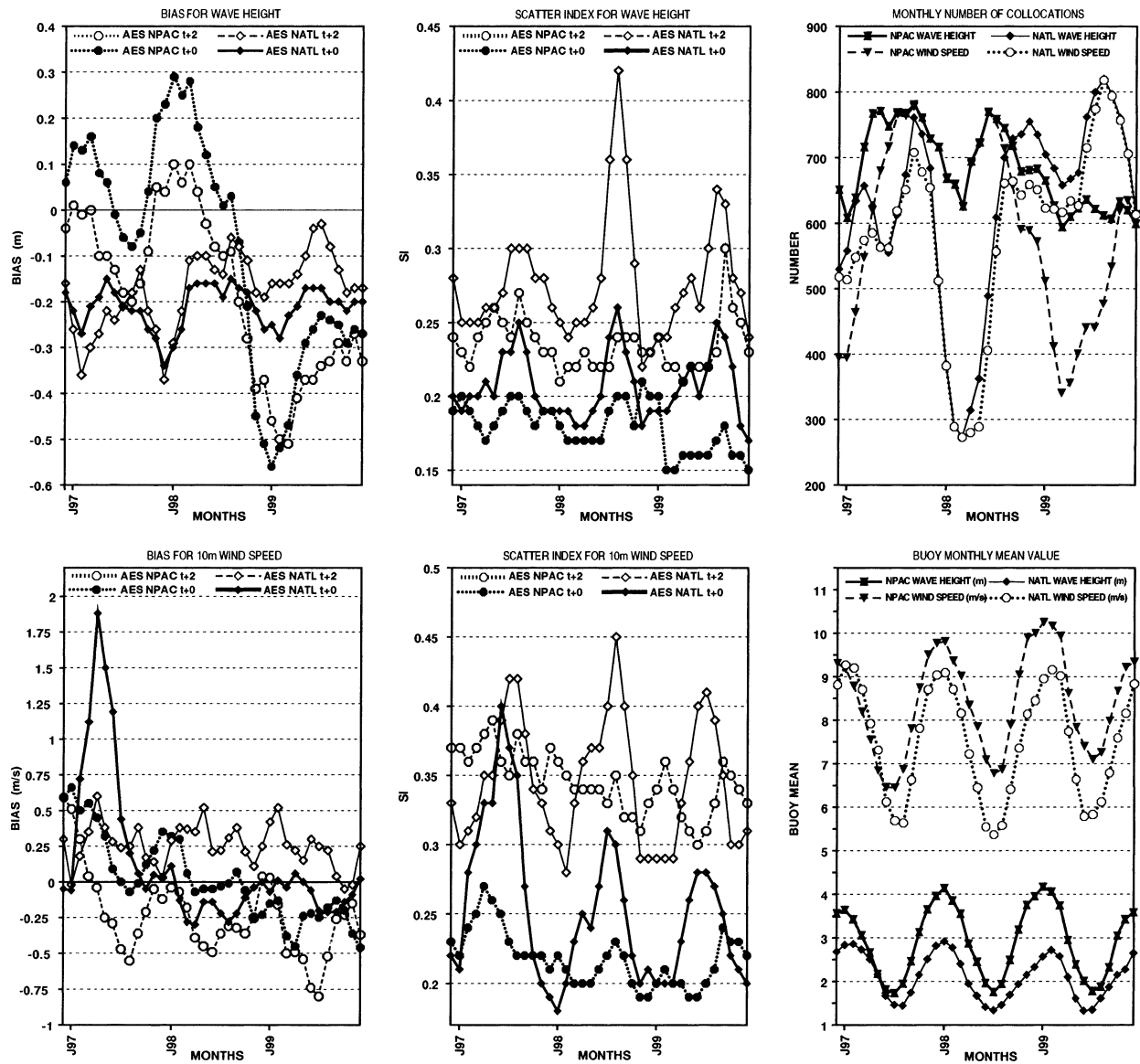


FIG. 7. Monthly time series of the AES analysis ($t + 0$) and day 2 forecast ($t + 2$) bias and scatter index for model wave heights and 10-m winds when compared with buoy data for the northeast Pacific area including the U.S. west coast (NPAC, dotted line with circles) and the northwest Atlantic area (NATL, solid line with diamonds) from Dec 1996 to Dec 1999. Buoy winds were adjusted to 10 m and a 3-month running average was used to smooth out the plots. Also shown are the mean buoy observations and the number of collocations between models and buoy. NPAC is defined as NPC and USEC, and NATL is defined as USEC and CANEC.

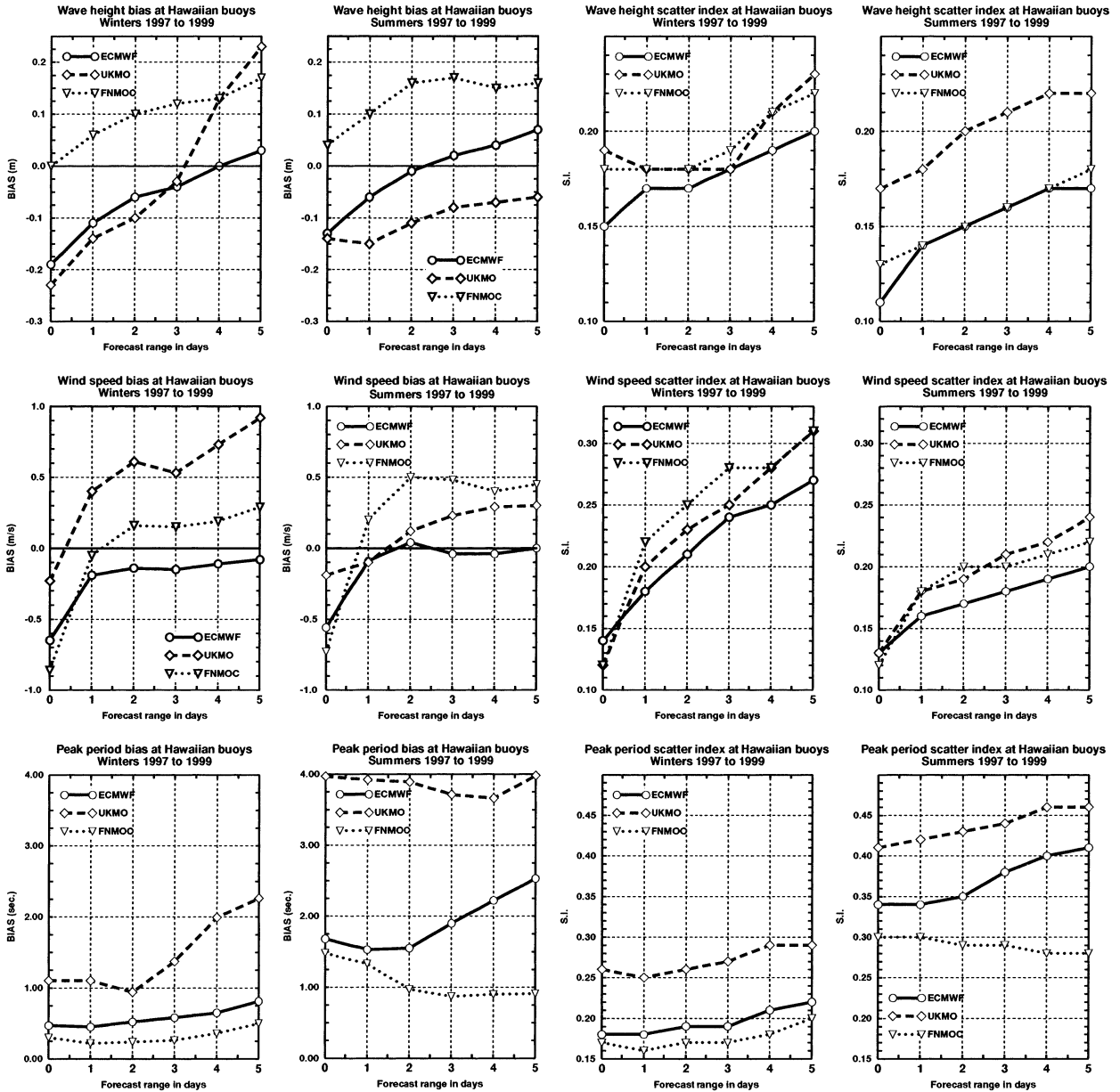
Group 1985, SWIM Group 1985) and even more recently by Fradon et al. (2000).

Even with the same original model (WAM), large differences still exist. The quality of the wind forcing is essential for the good performance of the wave model. It also determines to a large extent the evolution of the forecast errors (Janssen 1998). Nevertheless, some aspects of the respective implementations of WAM can be discussed.

The benefit of assimilating altimeter wave height (ECMWF, Met Office, NCEP) has been reevaluated by running a version of the ECMWF global wave model

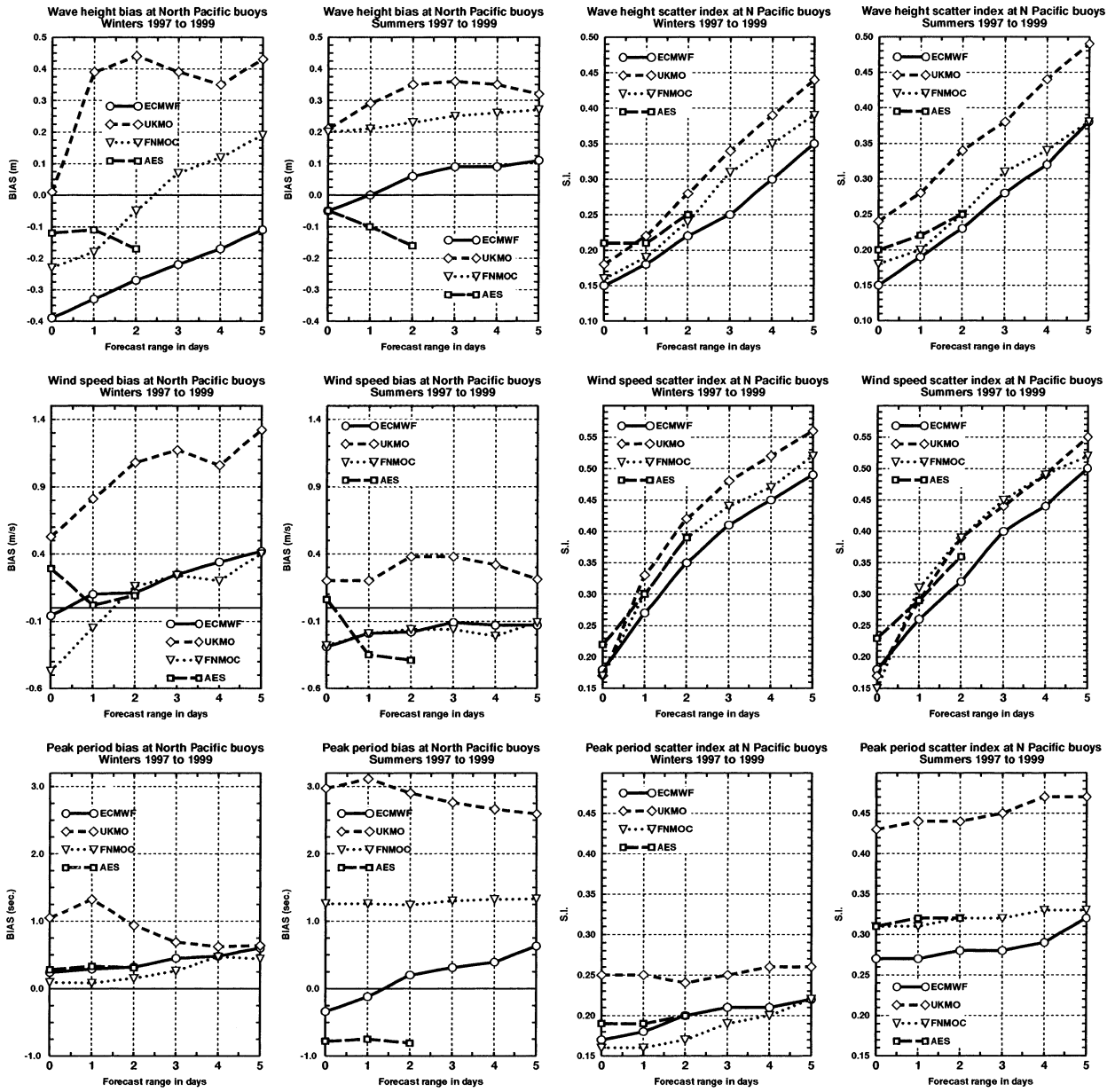
in an uncoupled mode with 6-hourly analyzed winds, with and without satellite data, for February and July 1999. The comparison with the buoy data indicates a net decrease in both systematic and random error (Table 7), confirming the advantage of such schemes.

It is known that wave spectral directional spreads have a tendency to be too broad, partly due to the limited number of directional bins used by the numerical models. An increase in angular resolution has a positive impact on the quality of the modeled waves. Table 8 displays the statistics for February 1999 of uncoupled analysis runs with the ECMWF model with, respectively,



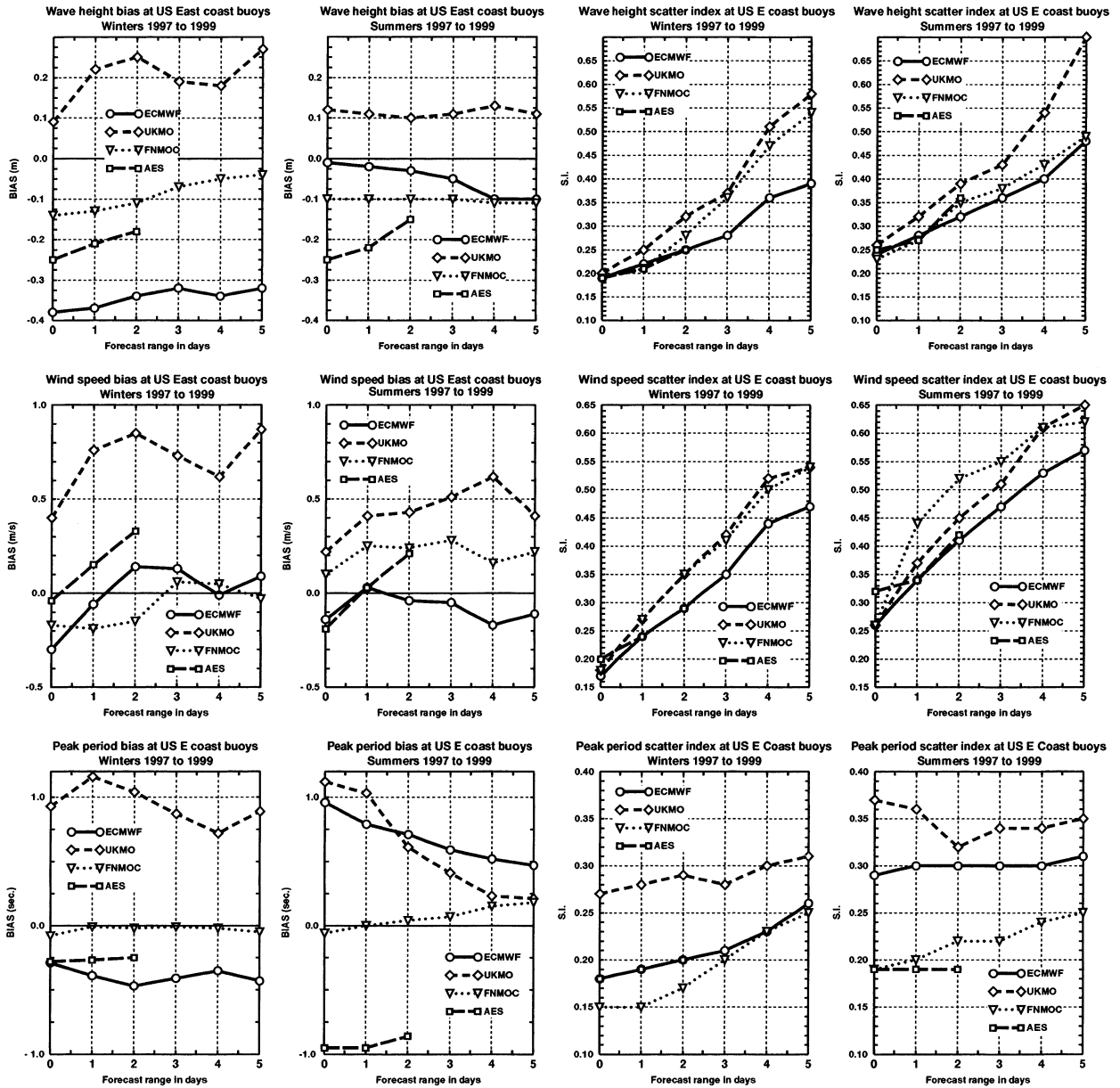
buoy statistics	number of entries in winter	winter mean	number of entries in summer	summer mean
wave height (m)	939	2.94	942	2.06
10m wind speed (m/s)	908	7.83	942	7.56
peak period (s)	911	11.74	941	8.81

FIG. 8. Winter and summer biases and scatter indices at the Hawaiian buoys as a function of forecast range for wave heights, 10-m wind speeds, and peak periods from ECMWF, Met Office, and FNMOG models for the period from Dec 1996 to Dec 1999. The mean values for each season are also given in the table at the bottom of the figure.



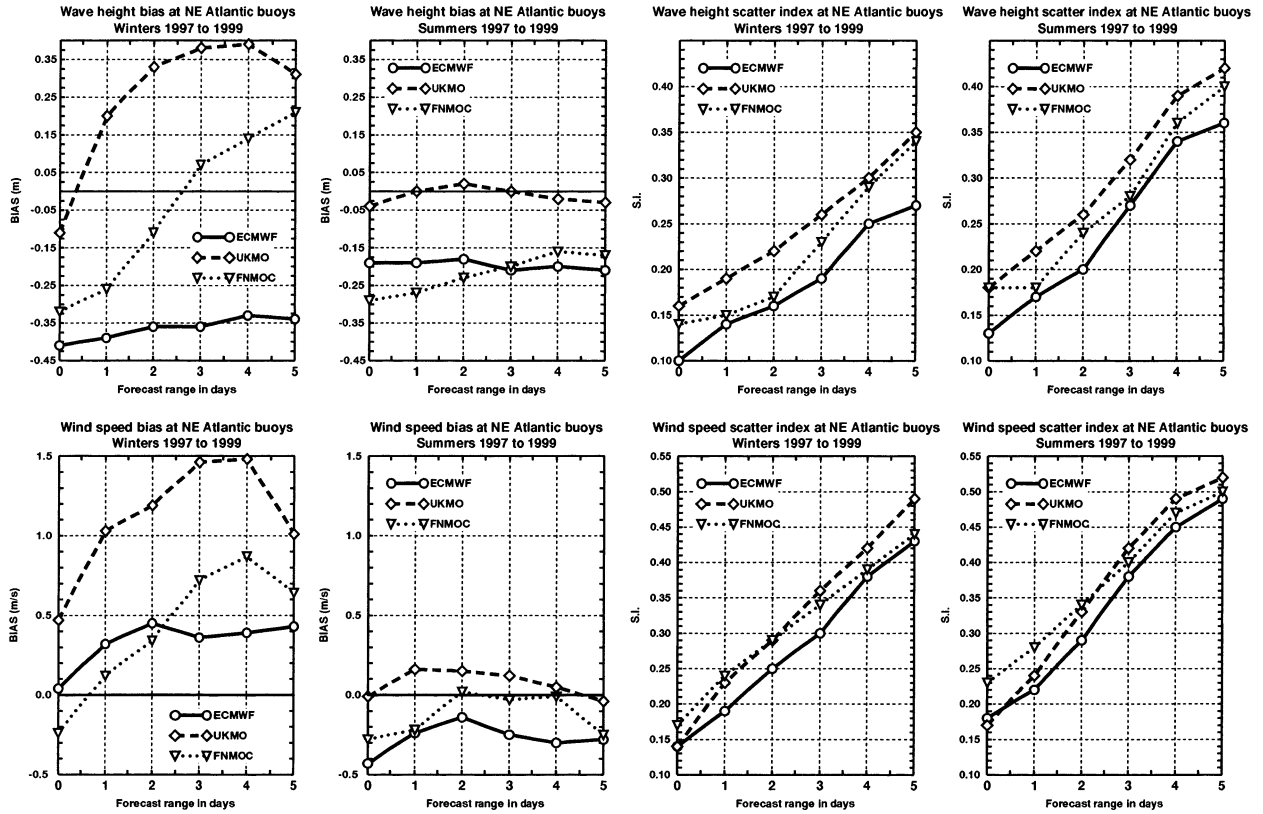
buoy statistics	number of entries in winter	winter mean	number of entries in summer	summer mean
wave height (m)	1165	3.88	1294	1.74
10m wind speed (m/s)	941	9.64	1202	6.70
peak period (s)	1159	11.31	1284	9.26

FIG. 9. Winter and summer biases and scatter indices at buoys in the northeastern Pacific area as a function of forecast range for wave heights, 10-m wind speeds, and peak periods from ECMWF, Met Office, FNMOC, and AES for the period from Dec 1996 to Dec 1999.



buoy statistics	number of entries in winter	winter mean	number of entries in summer	summer mean
wave height (m)	1052	2.44	1154	1.33
10m wind speed (m/s)	1020	8.68	1111	5.58
peak period (s)	1052	8.47	1150	7.34

FIG. 10. Winter and summer biases and scatter indices at buoys along the U.S. east coast as a function of forecast range for wave heights, 10-m wind speeds, and peak periods from ECMWF, Met Office, FNMOC, and AES for the period from Dec 1996 to Dec 1999.



buoy statistics	number of entries in winter	winter mean	number of entries in summer	summer mean
wave height (m)	968	4.55	1060	2.22
10m wind speed (m/s)	931	10.76	1036	7.52

FIG. 11. Winter and summer biases and scatter indices at buoys west of the British Isles as a function of forecast range for wave heights, 10-m wind speeds, and peak periods from ECMWF, Met Office, and FNMOC for the period from Dec 1996 to Dec 1999.

12, 18, and 24 directions. No altimeter data were used. Doubling the angular resolution does improve the wave model performance. This is, at first, unexpected because many sea observations of wind direction are truncated to the nearest of 16 directions. Hence, once a model resolution captures the observational directions it seems additional resolution would not matter much. However, the accuracy of swell propagation over large distances in models is critically controlled by angular resolution and hence this is likely a significant reason why we see improvements in the sea forecasts when angular resolution is improved. Following this recommendation, ECMWF increased its angular resolution from 12 to 24 in November 2000.

The buoy wind speed observations are included in the data used by the atmospheric data assimilation. However, those observations are generally assumed to be 10-m wind speeds and are thus assimilated without

any height correction. Figure 1 shows that most buoys carry an anemometer at around 5 m. All wind speed statistics presented so far were obtained by correcting the observed wind speeds using a logarithmic wind profile. A similar compilation can be done without any correction. For instance, Fig. 12 presents the difference between the binned bias statistics for observed wind speeds and their corrected counterparts (as in Fig. 6) for all buoys. Also shown are the differences between neutral winds at 5 or 7.5 m and the corresponding values at 10 m as derived from (1) and (2). Note that these differences are simply proportional to the friction velocity, which becomes a linear function of wind speed for large neutral winds. These differences can be interpreted as the maximum systematic bias that might be introduced by the analysis system when it tries to fit the model to the uncorrected wind observations. This problem might even get worse when the analysis scheme is

TABLE 7. Statistics from two runs of 1 month each of the stand-alone 0.5° ECMWF WAM with (with alt) or without (no alt) assimilation of altimeter wave heights. Statistics for wave heights (Hs) are given in the two left columns and those for peak periods (Tp) are in the two right columns. All runs were forced by 6-hourly winds from the ECMWF operational analysis.

Feb 1999	Hs no alt	Hs with alt	Tp no alt	Tp with alt
No. of entries	6829	6829	4243	4243
Buoy mean	2.80 m	2.80 m	9.35 s	9.35 s
Bias	-0.38 m	-0.22 m	-0.57 s	-0.08 s
Rmse	0.64 m	0.52 m	1.89 s	1.76 s
Scatter index	0.18	0.17	0.19	0.19
Symmetric slope	0.87	0.91	0.95	1.00
Jul 1999				
No. of entries	7486	7486	4525	4525
Buoy mean	1.31 m	1.31 m	7.40 s	7.40 s
Bias	-0.09 m	-0.01 m	0.64 s	1.07 s
Rmse	0.29 m	0.25 m	2.48 s	2.62 s
Scatter index	0.21	0.19	0.32	0.32
Symmetric slope	0.93	0.97	1.12	1.15

tailored to take into account hourly wind observations, as it is in the case of the ECMWF 4DVAR scheme. Although, this systematic bias may seem quite small, it may still result in a considerable bias in wave height. Starting from the equilibrium relation between wave height H_s and wind speed U_{10} (Komen et al. 1994),

$$H_s = \beta U_{10}^2/g, \quad (3)$$

where g is the acceleration of gravity and β is in general a function of U_{10} but in first approximation can be taken to be a constant (0.22) (Janssen et al. 1997). The wave height bias (δH_s) caused by a systematic wind bias (δU_{10}) can be estimated by

$$\delta H_s = (2\beta U_{10} \delta U_{10})/g. \quad (4)$$

This estimate is also plotted in Fig. 12 for each wind speed bias. For large wind speeds, the maximum wave height underestimation could be as large as 1 m. Note however that for large winds, the equilibrium hypothesis might not apply since those winds are usually associated with fast-moving weather systems. In section 4, we have also shown that analyzed wave heights for all WAM

configurations were sometimes significantly underestimated in the peaks of the time series. It is therefore reasonable to argue that some of these underestimations, when linked to local wave growth, might in part be explained by this systematic negative bias in analyzed wind speed.

In view of these results, there is no doubt that the actual anemometer height should be used to correct buoy wind speed observations. ECMWF has actually developed a corrective scheme for buoy and ship observations. It relies on a list of proper anemometer heights, which was put together by gathering information on ships and buoys. It uses the actual ocean boundary layer physics to adjust the observation to 10 m (D. Vasiljevic 1999, personal communication). The scheme has been in place since the end of June 2000 when a new operational cycle was introduced. A short experiment (9 days) shows the benefit of the corrective scheme (Table 9). The impact of this scheme is not as large as could be expected from Fig. 12; however, ship and buoy observations are usually not the only source of information in the vicinity of the buoys. Note also that buoy and

TABLE 8. Statistics from 1-month runs of the stand-alone 0.5° ECMWF WAM with different angular resolutions for the wave spectra. Statistics for wave heights (Hs) are given in the top section and those for peak periods (Tp) are in the bottom one. All runs were forced by 6-hourly winds from the ECMWF operational analysis and altimeter data were not used.

Hs Feb 1999	12 directions	18 directions	24 directions
No. of entries	6829	6829	6829
Buoy mean (m)	2.80	2.80	2.80
Bias (m)	-0.42	-0.41	-0.38
Rmse (m)	0.66	0.65	0.63
Scatter index	0.18	0.18	0.18
Symmetric slope	0.85	0.86	0.87
Tp Feb 1999			
No. of entries	4243	4243	4243
Buoy mean (s)	9.35	9.35	9.35
Bias (s)	-0.51	-0.50	-0.43
Rmse (s)	1.88	1.91	1.88
Scatter index	0.19	0.20	0.20
Symmetric slope	0.96	0.96	0.97

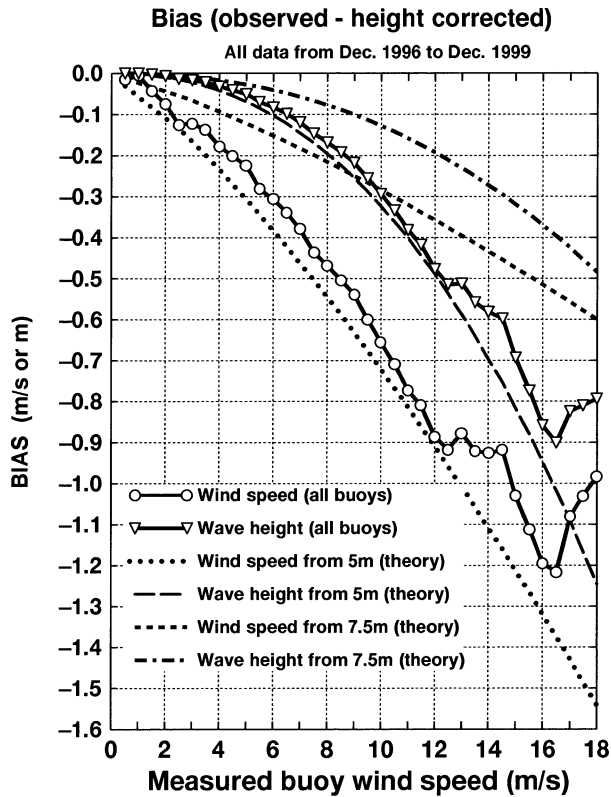


FIG. 12. The solid line with circles displays the difference between the 10-m wind speed bias (as in Fig. 6) and the bias that was obtained when the buoy data were not adjusted for the anemometer height (the actual observations). The solid line with triangles is derived from the previous relation using (4). The dotted line shows the difference in theoretical neutral wind speed at 5 and 10 m as a function of the wind speed at 5 m. The long-dashed line shows the corresponding bias in wave height according to (4), the short-dashed line is the wind speed difference between 7.5 and 10 m as a function of the wind at 7.5 m, and the dotted-dashed line is the corresponding bias in wave height according to (4).

ship wind speed data contain inherent truncation errors of $\pm 0.5 \text{ m s}^{-1}$. Last, the 4DVAR analysis error estimate of ship and buoy data might still be too large for those moored buoys equipped with high-quality anemometers. It is hoped that in the future the actual anemometer height and whether the wind observation was adjusted to 10 m will be included in the buoy data record. It will remove the need for a continual updating of a corrective list. Similarly, a higher precision of the reported wind measurements is desired if one wants to fully profit from these observations in a data assimilation of ever-increasing complexity.

6. Conclusions

Every month, wave model analyses and forecasts from five participating centers are compared with buoy observations at selected locations. The buoy data are obtained from the GTS and a basic quality control and averaging process is used to produce observed data that

TABLE 9. Buoy statistics for 9 days of the ECMWF coupled analysis system from 23 Mar 2000 to the end of Mar 2000. The reference is compared with a run in which wind speeds from buoys were adjusted to 10 m.

Wind, end of Mar 2000	Reference	Height corrected
No. of entries	1856	1856
Buoy mean (m s^{-1})	7.08	7.08
Bias (m s^{-1})	-0.34	-0.26
Rmse (m s^{-1})	1.47	1.47
Scatter index	0.20	0.20
Symmetric slope	0.95	0.96
Wave height, end of Mar 2000	Reference	Height corrected
No. of entries	2076	2076
Buoy mean (m)	2.10	2.10
Bias (m)	-0.22	-0.21
Rmse (m)	0.45	0.44
Scatter index	0.19	0.18
Symmetric slope	0.90	0.91

can be compared to the equivalent model values. The resulting statistics serve as an additional validation tool for the operational wave forecasting system (wind and waves) of each collaborating center. The comparison also provides a first insight into the performance of some of the main operational global wave forecasting systems with respect to each other.

It was shown that all global implementations of the third-generation Wave Model have a tendency to underpredict wave height when forced by analyzed wind fields (Fig. 6). On the other hand, it appears that besides using a different wave model, the Met Office system tends to have 10-m winds that are overestimated. The resulting wave analyses and forecasts in the areas where wave generation is important are therefore, in the mean, less underestimated; however, overpredictions occur more often. As a whole, the ECMWF system seems to perform the best, but there are regional differences. ECMWF appears to have more difficulties in representing wind and wave conditions on the western side of the ocean basins (U.S. east coast and Japan; Fig. 10). The comparison of the forecasting system at four of the five participating centers using the same original wave model (WAM) has also shown the essential importance of good-quality winds. Statistically, the center with the lowest forecast wind errors (ECMWF) also has the lowest wave forecast errors. It is also apparent that some research is still needed to address some of the systematic wave height underestimation without boosting the model winds well above the observed values.

Looking back at some of the differences in the implementation of WAM indicates the positive impact of assimilating altimeter wave heights. It also illustrates the benefit of an increase in angular resolution of the discretized wave spectrum.

Because of the design of the meteorological buoys, wave, and also wind, data are reported. It was argued

that since buoy winds are not corrected for the actual height of the anemometers, a systematic bias might be present in the wind analysis, which in turn could explain some of the analyzed wave height underestimation. Effort should be made to adjust the wind data before they can be used by the model assimilation as is now done at ECMWF. It is also desirable that the high quality of the buoy winds is not truncated in the encoding to GTS.

It is believed that centers engaged in wave forecasting and their product users will benefit from this activity in the same way that weather centers benefit from the exchange of forecast verification scores. Everyone involved in the project knows the actual skill of the model forecasts and sees what kinds of shortcomings still exist. Ultimately it could lead to improvements in future wave models. Other operational centers are encouraged to join (Météo-France joined at the beginning of 2001).

It is hoped that by making the information widely available, it will stimulate a more comprehensive exchange of wave data among organizations that collect wave data but do not make them available on GTS.

Acknowledgments. Careful reading and constructive comments by Peter Janssen and Martin Miller are gratefully acknowledged. We also thank the reviewers for their thorough reviews and their constructive comments on how to improve the quality of the paper.

REFERENCES

- Bauer, E., and C. Staabs, 1998: Statistical properties of global significant wave height and their use for validation. *J. Geophys. Res.*, **103C**, 1153–1166.
- Bengston, L., 1999: From short-range barotropic modelling to extended-range global weather prediction: A 40 year perspective. *Tellus*, **51AB**, 13–32.
- Bidlot, J.-R., and M. Holt, 1999: Numerical wave modelling at operational weather centres. *Coastal Eng.*, **37**, 409–429.
- , P. Janssen, B. Hansen, and H. Günther, 1997: A modified set up of the advection scheme in the ECMWF wave model. ECMWF Tech. Memo. 237, ECMWF, Reading, United Kingdom, 31 pp.
- , M. Holt, P. A. Wittmann, R. Lalbeharry, and H. S. Chen, 1998: Towards a systematic verification of operational wave models. *Proc. Third Int. Symp. on Ocean Wave Measurement and Analysis: WAVES97*, Virginia Beach, VA, American Society of Civil Engineers, 653–667.
- , D. J. Holmes, P. A. Wittmann, R. Lalbeharry, and H. S. Chen, 2000: Intercomparison of the performance of operational ocean wave forecasting systems with buoy data. ECMWF Tech. Memo. 315, ECMWF, Reading, United Kingdom, 46 pp.
- Bouws, E., G. J. Komen, R. A. van Moerkerken, H. H. Peeck, and M. J. M. Saraber, 1986: An evaluation of operational wave forecasts on shallow water. *Wave Dynamics and Radio Probing of the Ocean Surface*, O. M. Phillips and K. Hasselmann, Eds., Plenum Press, 639–660.
- , D. Jannink, and G. J. Komen, 1996: On the increasing wave height in the North Atlantic Ocean. *Bull. Amer. Meteor. Soc.*, **77**, 2275–2277.
- Cardone, V. J., 1987: The present status of operational wave forecasting. *Johns Hopkins APL Tech. Dig.*, **8**, 24–32.
- Charnock, H., 1955: Wind stress on a water surface. *Quart. J. Roy. Meteor. Soc.*, **81**, 639–640.
- Chen, H. S., 1995: Ocean surface waves. TPB 426, NOAA/NWS/OM, 18 pp.
- Clancy, R. M., J. E. Kaitala, and L. F. Zambresky, 1986: The Fleet Numerical Oceanography Center Global Spectral Ocean Wave Model. *Bull. Amer. Meteor. Soc.*, **67**, 498–512.
- Côté, J., J. G. Desmarais, S. Gravel, A. Methot, A. Patoine, M. Roch, and A. Staniforth, 1998a: The operational CMC-MRB Global Environmental Multiscale (GEM) model. Part II: Results. *Mon. Wea. Rev.*, **126**, 1397–1418.
- , S. Gravel, A. Methot, A. Patoine, M. Roch, and A. Staniforth, 1998b: The operational CMC-MRB Global Environmental Multiscale (GEM) model. Part I: Design considerations and formulation. *Mon. Wea. Rev.*, **126**, 1373–1395.
- Fradon, B., D. Hauser, and J.-M. Lefèvre, 2000: Comparison study of a second-generation and of a third-generation wave prediction model in the context of the SEMAPHORE Experiment. *J. Atmos. Oceanic Technol.*, **17**, 197–214.
- Gauthier, P., C. Charette, L. Fillion, P. Koclas, and S. Laroche, 1999: Implementation of a 3D variational data assimilation system at the Canadian Meteorological Centre. Part I: The global analysis. *Atmos.–Ocean*, **37**, 103–156.
- Golding, B., 1983: A wave prediction system for real time sea state forecasting. *Quart. J. Roy. Meteor. Soc.*, **109**, 393–416.
- Günther, H., G. J. Komen, and W. Rosenthal, 1984: A semi-operational comparison of wave prediction models. *Dtsch. Hydrogr. Z.*, **37**, 89–106.
- Hogan, T. E., and T. E. Rosmond, 1991: The description of the U.S. Navy Operational Global Atmospheric Prediction System's Spectral Forecast Model. *Mon. Wea. Rev.*, **119**, 1786–1815.
- Holt, M. W. 1994: Improvement to the UKMO wave model swell dissipation and performance in light winds. Met Office Forecasting Research Division Tech. Rep. 119, 12 pp.
- , 1997: Assimilation of ERS-2 altimeter observations into a global wave model. *Research Activities in Atmospheric and Oceanic Modelling—1997*, WGNP Rep. 25, WMO/TD-792, 8.31–8.32.
- Janssen, P. A. E. M., 1989: Wave-induced stress and the drag of air flow over sea. *J. Phys. Oceanogr.*, **19**, 745–754.
- , 1991: Quasi-linear theory of wind wave generation applied to wave forecasting. *J. Phys. Oceanogr.*, **21**, 1631–1642.
- , 1998: On error growth in wave models. ECMWF Tech. Memo. 249, ECMWF Reading, United Kingdom, 12 pp.
- , 2000: Wave modeling and altimeter wave height data. *Satellites, Oceanography, and Society*, D. Halpern, Ed., Elsevier Science, 35–56.
- , B. Hansen, and J.-R. Bidlot 1997: Verification of the ECMWF wave forecasting system against buoy and altimeter data. *Wea. Forecasting*, **12**, 763–784.
- , J.-R. Bidlot, and B. Hansen, 2000a: Diagnosis of ocean-wave forecasting systems. *Proc. Seminar on Diagnostics of Models and Data Assimilation Systems*. Reading, United Kingdom, ECMWF, 233–256.
- , J. D. Doyle, J. Bidlot, B. Hansen, L. Isaksen, and P. Viterbo, 2000b: Impact of ocean waves on the atmosphere. *Proc. Seminar on Atmosphere–Surface Interaction*, Reading, United Kingdom, ECMWF, 85–111.
- Khandekar, M. L., and R. Lalbeharry, 1996: An evaluation of Environment Canada's operational wave model based on moored buoy data. *Wea. Forecasting*, **11**, 139–152.
- Komen, G. J., L. Cavaleri, M. Donelan, K. Hasselmann, S. Hasselmann, and P. A. E. M. Janssen, Eds., 1994: *Dynamic and Modelling of Ocean Waves*. Cambridge University Press, 532 pp.
- Laroche, S., P. Gauthier, J. St-James, and J. Morneau, 1999: Implementation of a 3D variational data assimilation system at the Canadian Meteorological Centre. Part II: The regional analysis. *Atmos.–Ocean*, **37**, 281–307.
- Lionello, P., H. Günther, and P. A. E. M. Janssen, 1992: Assimilation of altimeter data in a global third generation wave model. *J. Geophys. Res.*, **97C**, 14 453–14 474.
- Monaldo, F., 1988: Expected difference between buoy and radar altimeter estimates of wind speed and significant wave height and

- their implications on buoy–altimeter comparisons. *J. Geophys. Res.*, **93C**, 2285–2302.
- Ritchie, H., and C. Beaudoin, 1994: Approximations and sensitivity experiments with a baroclinic spectral model. *Mon. Wea. Rev.*, **122**, 2391–2399.
- Romeiser, R., 1993: Global validation of wave model WAM over a one year period using Geosat wave height data. *J. Geophys. Res.*, **98C**, 14 453–14 474.
- Smith, S., 1988: Coefficients for sea surface wind stress, heat flux and wind profiles as a function of wind speed and temperature. *J. Geophys. Res.*, **93C**, 15 467–15 472.
- Sterl, A. G., G. J. Komen, and P. D. Cotton, 1998: Fifteen years of global wave hindcasts using ERA winds: Validating the reanalysed winds and assessing the wave climate. *J. Geophys. Res.*, **103C**, 5477–5492.
- SWAMP Group, 1985: An intercomparison study of wind wave prediction models, part 1: Principal results and conclusions. *Ocean Wave Modelling*, Plenum Press, 3–153.
- SWIM Group, 1985: Shallow Water Intercomparison of Wave Prediction Models (SWIM). *Quart. J. Roy. Meteor. Soc.*, **111**, 1087–1113.
- Tolman, H. L., 1999: User manual and system documentation of WAVEWATCH-III version 1.18. NOAA/NWS OMB Contribution No. 166, 110 pp.
- Wittmann, P. A., and R. M. Clancy, 1994: Implementation and validation of a global third-generation wave model. *Ocean Wave Measurement and Analysis: Proc. of the Second International Symposium*, O. T. Magoon and J. M. Hemsley, Eds., American Society of Civil Engineers, 406–419.
- , and T. C. Pham, 1999: Coastal wave predictions forced by mesoscale winds. Preprints, *Third Conf. on Coastal Atmospheric and Oceanic Prediction Processes*, New Orleans, LA, Amer. Meteor. Soc., 113–115.
- , R. M. Clancy, and T. Mettlach, 1995: Operational wave forecasting at Fleet Numerical Meteorology and Oceanography Center, Monterey, CA. Environment Canada, Preprints, *Fourth Int. Workshop on Wave Hindcasting and Forecasting*, Banff, AB, Canada, Atmospheric Environment Service, 335–342.
- Zambresky, L., 1987: The operational performance of the Fleet Numerical Oceanography Center global spectral ocean-wave model. *Johns Hopkins APL Tech. Dig.*, **8**, 33–36.
- , 1989: A verification study of the global WAM model. December 1987–November 1988. ECMWF Tech. Rep. 63, ECMWF, Reading, United Kingdom, 86 pp.